Upscaling And Consistent Sialylation Of Plant Produced Antibodies

Flávio da Silva Amaro Sádio

Dissertação para a obtenção do Grau de Mestre em

Engenharia Agronómica

Orientador: Dra. Wanda Viegas
Dra. Herta Steinkellner
Dra. Alexandra Castilho

Júri:
Presidente: Doutora Cristina Maria Moniz Simões Oliveira, Professora Associada com agregação do(a) Instituto Superior de Agronomia da Universidade de Lisboa
Vogais: Doutora Maria Wanda Sarujine Viegas, Professora Catedrática do(a) Instituto Superior de Agronomia da Universidade de Lisboa
Doutora Sara Barros Queiroz Amâncio, Professora Associada com agregação do(a) Instituto Superior de Agronomia da Universidade de Lisboa

2015

Acknowledgements

I would like to thank firstly Ana Caperta and Wanda Viegas for giving me the possibility to do my thesis abroad with the Steinkellner Group. I also thank you for the support you gave me through my collaboration with you, and of course for the knowledge you passed on to me so dearly.

I also want to thank Herta Steinkellner and Alexandra Castilho for the warm welcome you gave me in your group, for all the knowledge and help during the first times, and the patience that you displayed with me, of course.

For all my lab mates through all these years, I thank the practical experience you shared with me, as well as the fun times we had. Trust me I could not have done it without all of you (and this means Thomas Hackl, Somanath Kallolimath, Michaela Bogner, Diana Tomás, Joana Firmino, Ana Patrícia Avó, Raimundo Diz and others that i may not remember now, but should know they were a main part of this).

A very special thank you to Ana Sofia Róis. You were the single most responsible for teaching me lab work, discipline, competence, and every other quality needed for this work. This proves that sometimes you need a bit of tough love.

I also want to mention my family and friends in Portugal and Vienna, for the support given even when i may have been a little careless. While far away, i still did not forget you all.

Another thank you goes to Nataliia Konstantinova. You helped me with the loneliness and always motivated me to do just a little bit more.

My acknowledgements also go to Richard Strasser, Yunji Shin, Friedrich Altmann and Clemens Gruber for the technical support during my thesis.

Finally, I want to thank all the entities responsible for allowing me to do my thesis: ISA, the University of Lisbon, BOKU Wien, Icon Genetics and the European Comission for the possibility to enter the Erasmus Program.

Resumo: Uma grande parte dos produtos biofarmacêuticos são glicoproteínas. Para a sua produção, é necessário atingir um nível elevado de homogenia a nível da estrutura proteica, mas também dos glicanos ligados à proteína produzida, uma vez que influenciam a sua função. Para atingir este objectivo, as plantas surgem como a plataforma ideal de produção de biofarmacêuticos. Infiltrando folhas de plantas adultas com uma suspensão de *Agrobacterium tumefaciens* contendo um plasmídeo em que se insere o gene do produto desejado, é possível produzir uma quantidade elevada de proteína num período bastante curto.

Neste estudo foi estabelecida a produção em larga escala de dois anticorpos, Rituximab e KBPA, como representantes das famílias de Imunoglobulinas G e M, em *Nicotiana benthamiana* geneticamente modificada para alterar os padrões de glicosilação de proteínas. Adicionalmente, a co-infiltração dos genes para estes anticorpos com genes que codificam glicosiltransferases, permitiu obter estruturas específicas de glicanos ligados a estas proteínas. Finalmente, foi também descrita a inibição da expressão de β-N-acetilhexosaminidase 3 com recurso a RNAi, diminuindo o efeito desta glicosidase nos glicanos de proteínas produzidas por plantas.

Palavras-Chave: *Nicotiana benthamiana*; Engenharia de glicanos; Produtos biofarmacêuticos; Anticorpos; RNAi

Abstract: Glycoproteins are a major part of biopharmaceutical products. For their production, a high level of homogeny is required, not only for the protein but also for attached glycans, since these oligossacharides influence protein function. For this goal, plants emerge as an ideal biopharmaceutical production platform. By infiltrating adult plant leaves with a suspension of *Agrobacterium tumefaciens* containing a plasmid for the gene of interest, a high amount of protein can be produced in a short period.

In this study, the production of two antibodies in genetically glycoengineered *Nicotiana benthamiana* was described. These antibodies, Rituximab and KBPA, served as models for Immunoglobulin groups G and M. Additionally, co-infiltration of the genes for these antibodies with glycoengineering constructs allowed for specific glycan structures attached to these proteins. Finally, the down-regulation of β-N-acetylhexosaminidase 3 with RNAi technology was described, inhibiting the effect of this glycosidase on plant produced proteins.

Keywords: *Nicotiana benthamiana*; Glycoengineering, Biopharmaceutical products, Antibodies, RNAi

Resumo Alargado: Os produtos biofarmacêuticos constituem uma importante e crescente parte da indústria farmacêutica. Actualmente, a maior parte destes produtos e produzida com recurso a linhas celulares como CHO. No entanto, a procura de plataformas alternativas é necessária. Como resposta a esta procura, as plantas representam uma alternativa viável, permitindo a redução de custos de produção, mas também aumentando a quantidade de produto produzido e a segurança, uma vez que as plantas não possuem os agentes patogénios típicos de humanos ou sequer mamíferos.

Com recurso a Magnifection, uma tecnologia desenvolvida pela Icon Genetics, que combina vectores virais com a infecção por *Agrobacterium tumefaciens*, é possível infiltrar os tecidos de uma planta com uma suspensão desta bactéria modificada e produzir uma determinada proteína. Os vectores virais modificados inseridos na cultura de bactérias contêm os genes de interesse necessários à produção de proteínas e, inseridos no núcleo celular das plantas, utilizam a sua maquinaria para a síntese proteica.

Outro factor importante é a glicosilação de glicoproteínas produzidas por este modo. Uma vez que os glicanos influenciam a função das proteínas, é importante que sejam produzidas proteínas com glicanos optimizados para o efeito. De facto, o impacto das estruturas de glicanos em anticorpos influencia a interacção dos anticorpos com os seus receptores nas células efectoras. Do mesmo modo, as plantas produzem glicosidases que podem modificar os glicanos das proteínas produzidas.

Este estudo teve como objectivo a produção em larga escala de anticorpos, Rituximab e KBPA, homogenicamente glicosilados. Os genes para as cadeias destes anticorpos, introduzidos na planta com recurso à tecnologia acima descrita, permitiram a produção das proteínas em *Nicotiana benthamiana*. Além da produção de proteínas, foi também promovida a costumização da estrutura glicosídica dos glicanos. De acordo com a estrutura glicosídica pretendida, folhas de *N. benthamiana* foram co-infiltradas com sequências para os anticorpos e vectores binário contendo sequências para controlar a glicosilação. Estas permitiram que os anticorpos produzidos em plantas possuíssem não só os mesmos glicanos que aqueles observados em anticorpos humanos, mas também formas optimizadas para o teste de funções específicas, como a propriedade anti-inflamatória de Rituximab.

Finalmente, foi obtida a inibição da actividade da enzima β-N-acetilhexosaminidase 3 pela síntese de um inserto de RNAi para a sequência da mesma. A actividade desta glicosidase abrange algumas proteínas segregadas para o apoplasto das células vegetais. Como este é muitas vezes o caminho das proteínas recombinantes produzidas em plantas, torna-se interessante o silenciamento da actividade desta enzima, de modo a evitar que degrade a estrutura glicosídica dos glicanos.

List of Figures:

Abbreviations:

A1AT, alpha-1 anti-trypsin; **AA**, terminal galactosylated glycoform; **CHO**, chinese hamster ovary cells; **CMAS**, human CMP-N-acetylneuraminic acid synthase; **ER**, endoplasmatic reticulum; **Fab**, fragment antigen-binding; **Fc**, fragment crystallizable; **FucT**, α1,3-fucosyltransferase; **GalT**, Galactosyltransferase; **Glc**, glucose; **GlcNAc**, *N*-acetylglucosamine; **GMP**, good manufacturing practice; **GNE**, mouse UDP-N-acetylglucosamine 2-epimerase/N-acetylmannosamine-kinase; **GnGn**, terminal *N*-acetylglucosamine glycoform; **GnGnF^3**, terminal *N*-acetylglucosamine glycoform with α1,3 core fucose; **GnGnXF^3**, terminal *N*-acetylglucosamine glycoform with α1,3 core fucose and β1,2 core xylose; **HC**, heavy chain; **HEXO 1**, hexosaminidase 1; **HEXO 3**, hexosaminidase 3; **HIV**, human immunodeficiency virus; **IgG**, immunoglobulin G; **IgM**, immunoglobulin M; **LC**, light chain; **LC-ESI-MS**, liquid chromatography electrospray ionization mass spectrometry; **mAb**, monoclonal antibody; **Man**, mannose; **Man5**, glycoform with five mannose residues; **Man8**, glycoform with eight mannose residues; **MMX**, paucimannosidic glycoform with β1,2 core xylose; **MMXF^3**, paucimannosidic glycoform with α1,3 core fucose and β1,2 core xylose; **NaNa**, terminal sialic acid glycoform; **NaNaF^3**, terminal sialic acid glycoform with α1,3 core fucose; **NANS**, human N-acetylneuraminic acid phosphate-synthase; **Neu5Ac**, *N*-acetylneuraminic acid (sialic acid); **PVX**, potato virus X; **RT**, room temperature; **Rx**, rituximab; **ST**, sialyltransferase; **TMV**, tobacco mosaic virus; **TSP**, total soluble proteins; **ΔXF** *N. benthamiana* glycosylation mutants lacking the core α1,3 fucose and β1,2 xylose residues; **XylT**, α1,2-xylosyltransferase

Table of Contents

1 Introduction

1.1 Plants as a protein production platform

The biopharmaceutical industry is today a billion dollar business with ever increasing demand by the world market, and recombinant proteins like antibodies and antibody derived products being the most sought after (Loos and Steinkellner, 2014).

Due to the desirability of these products, efforts have been made to further develop recombinant protein expression platforms, like bacteria, insect, yeast or mammalian cell cultures, with the last being the most popular. These platforms, though widely used, show some limitations in terms of production costs, time, product flexibility, and safety from contamination. Because of these factors, worldwide availability and the ability to tackle global health issues is still low for biopharmaceuticals (Whaley et al., 2011).

Plants represent an alternative expression platform with a high potential, allowing for cost efficient and safe production of recombinant proteins (Werner et al., 2011), along with easy upscalability, high product flexibilty and reduced production time (Gleba et al., 2014). Additionally, in this reduced production time, great quantities of protein can be produced (Giritch et al., 2006).

In fact, due to the possibility of transient gene expression in plants, a protein of interest can be agro-infiltrated, expressed and purified in a plant like *Nicotiana benthamiana* on a period from 3-8 days (Klimyuk et al., 2014).

Recently, this expression platform has been used for researching the production of antibodies (Whaley et al., 2011), enzymes (Schneider et al., 2014a), hormones (Dirnberger et al., 2001), vaccines (Rybicki, 2010) or growth factors (Musiychuk et al., 2013), for instance.

As an industrially viable platform, plants are still in the beginning phase, although there are already several companies with GMP manufacturing sites around the world to produce plant-derived bioproducts (Stoger et al., 2014). Also, in 2013, the FDA approved the first plant derived molecular pharming product, Elelyso^{TM}. This is the plant derived taligluciferase alpha, used to treat Gaucher's disease, produced and distributed by Protalix Biotherapeutics (Shaaltiel et al., 2007).

Such developments come to show that plants as industrial protein production platforms are growing in popularity, which also means that plant-products quality it at least as good as the conventional recombinant protein expression platforms, safe for consumption and economically competitive.

1.2 *N*-Glycosylation

Most human proteins are glycosylated (Apweiler et al., 1999). This means oligosaccharide side chains attached to specific amino acids in a defined sequence (figure 1, (Wang et al., 2012)). Also, the majority of FDA approved biochemical drugs are glycosylated (Aggarwal, 2011).

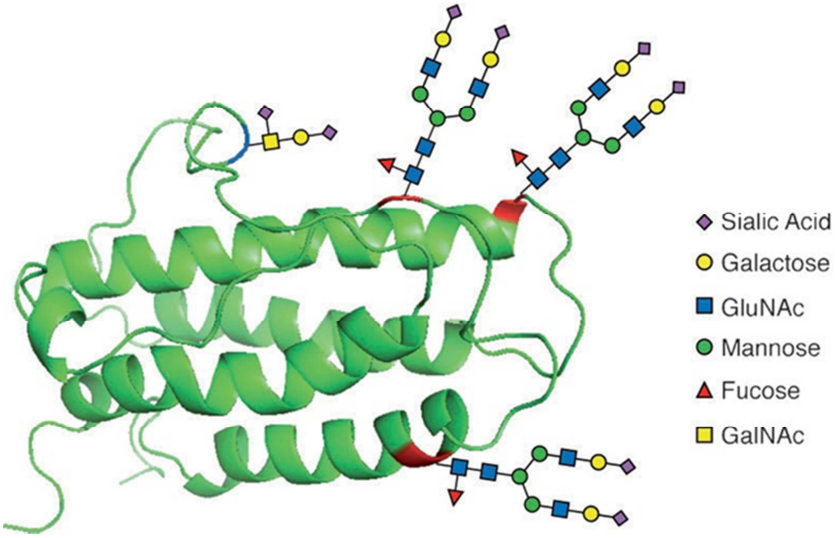

Figure 1: Erythropoietin molecule with attached *N* and *O* glycans.

Glycosylation is a generally conserved post translational modification in most eukaryotic organisms, and is not regulated by a template like DNA or protein synthesis, but rather by the availability of sugar substrates, glycosylation proteins and their competition for available substrate (Schwarz and Aebi, 2011).

One type of glycosylation is *N*-glycosylation, happening in an asparagine residue of a consensus Asn-X-Ser/Thr sequence (with X being any amino acid but proline). Therefore, the number of glycosylation sites is dependent on the amino acid sequence of the protein and the availability of these due to the conformation of the protein.

The glycosylation process starts in the ER, with the synthesis of the precursor oligosaccharide, transfer to the target protein and initial trimming of sugar residues until a Man8 structure is obtained (see review in (Nagels et al., 2012)). It consists of two core GlcNAcs attached to a mannose, which then connects to two branches of additional mannose. On this phase, yeast-like glycosylation branches away from the other eukaryote organisms' glycosylation process, by adding more mannose to the Man8 structure, while other organisms transport the protein into the *cis*-Golgi and further trim down this glycan to a Man5 (figure 2).

While the protein moves through the Golgi, two more mannoses are removed, and two GlcNAcs are added to the *N*-glycans. This core structure (GnGn) formed in the *medial*-Golgi is the last common structure between mammals and plants. In insects, only one

branch GlcNAc is added, and then removed. Two core fucoses can be added in α1,3- and α1,6- linkage to the first core GlcNAc (figure 2) (Shi and Jarvis, 2007). Mammals can add galactose in β1,4- linkage to each of the branch GlcNAc and at the same time, a fucose in α1,6- linkage to the first core GlcNAc. The branches can also be extended by the addition of Neu5Ac to each of the branches in α2,3- or α2,6- linkage (figure 2). Plants do not process the GnGn structure the same way. First, a xylose is added in β1,2- linkage to the core mannose, followed by a fucose in α1,3- linkage to the first core GlcNAc (figure 2). The branches can also be extended by the addition of α1,3- linked galactose and α1,4- linked fucose, forming Lewis-A motifs (see review (Nagels et al., 2012)).

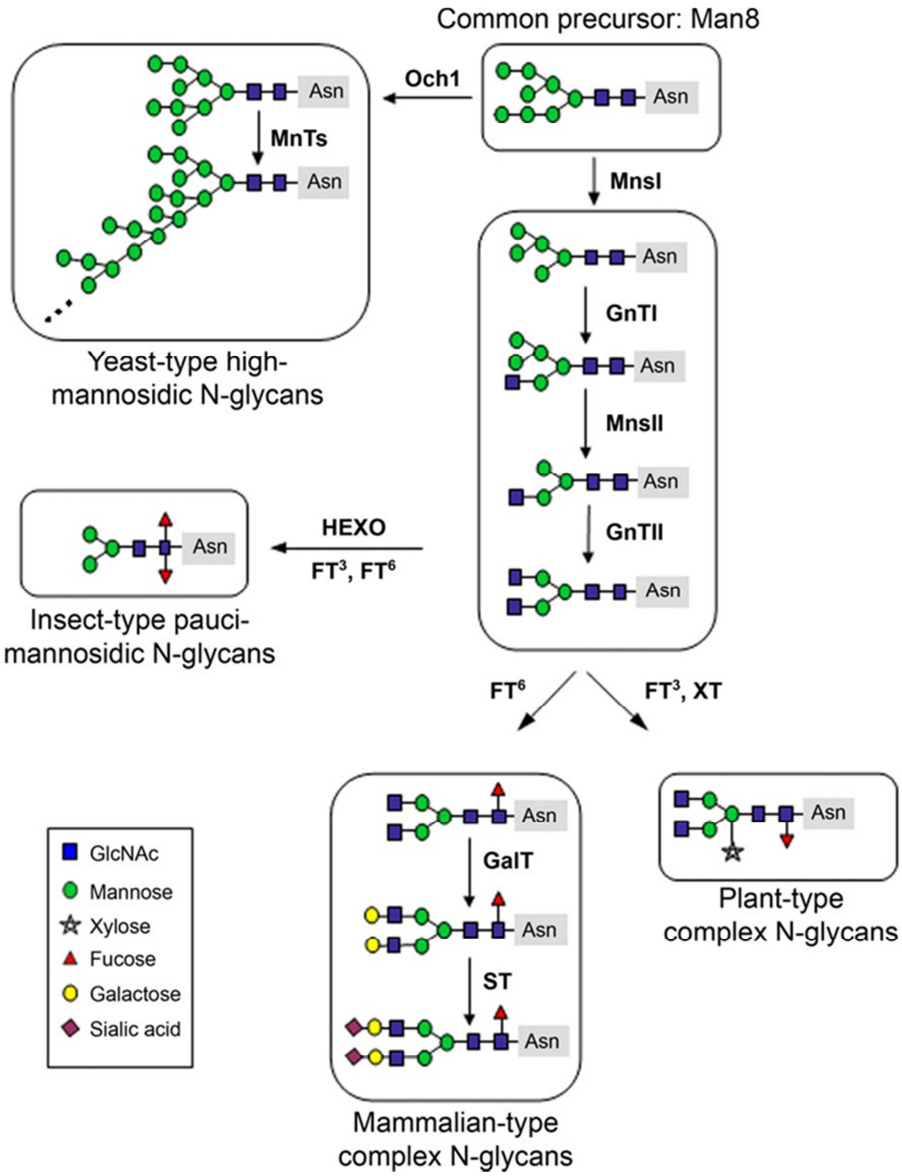

Figure 2: Different N-glycosylation pathways according to different organism groups. Och1: α1,6-mannosyltransferase; MnTs: mannosyltransferases; Mns: mannosidase; GnT: N-acetylglucosaminyltransferase; GalT: α1,4-galactosyltransferase; ST: α2,6-sialyltransferase; HEXO: hexosaminidase (N-acetylglucosaminidase); XT: β 1,2-xylosyltransferase; FT3: core fucosyltransferase in α1,3-linkage; FT6 : core fucosyltransferase in α1,6-linkage. Adapted from (Loos and Steinkellner, 2012).

N-glycosylation is an important factor for the quality of recombinant protein production. It influences folding of the protein in the ER (Varki, 1993), and later the stability, solubility, activity (Roth et al., 2010; Sola and Griebenow, 2010), subcellular targeting and immunogenicity. Therefore, it is important for the recombinant protein industry to achieve glycosylation patterns that optimize protein quality and also mimic the human-like glycosylation process.

1.2.1 Achieving human-like *N*-glycosylation in plants

Human serum proteins can have an immense degree of heterogeneity in glycosylation patterns. It has even been noticed for human serum IgG antibodies to have different glycosylation patterns in distinct physiological circumstances (Hasnat et al., 2007). Hence, for recombinant protein production in plants, this platform has to be able to express proteins with glycan homogeneity, and with flexibility to produce different kinds of glycans when needed.

Since plants lack the ability to produce mammal-like complex glycans, are poor in complex glycan structures (Strasser et al., 2014) and their non-human epitopes can have immunogenic activity (Bardor et al., 2003), this could pose a problem on this production platform.

Fortunately, glycoengineering is a solution. Plants are highly susceptible to glycoengineering (Strasser et al., 2014), and in general do not display a noticeable phenotype when modified for the purpose of changing glycan structures (Strasser et al., 2004; Strasser et al., 2008).

Therefore, by glycoengineering, plant produced recombinant proteins can have human like glycans and so be eligible for pharmaceutical purposes (see review in (Steinkellner and Castilho, 2015)).

The first advances towards mimicking human-like glycan structures in plants were made in *Arabidopsis thaliana* plants. Mutant lines were created by knockout of XylT and FucT genes (Strasser et al., 2004). This mutation was able to generate endogenous proteins with highly homogenized GnGn glycan profiles, making up for over 40 % of the total glycans. Also, mAbs produced in this line showed homogenous glycan structures, with GnGn being the most common structure, about 75 % of total glycans (Schahs et al., 2007). Since *A. thaliana* is not economically viable for the production of recombinant proteins, especially due to its low biomass, the stable knockout of XylT and FucT was attempted in other species (see review in (Steinkellner and Castilho, 2015)).

In *N. benthamiana*, the ΔXF line was generated by RNAi down regulation (figure 3) (Strasser et al., 2008). MAbs expressed in this platform showed profiles of 90 % GnGn

glycans, without xylose or fucose residues (Strasser et al., 2008), and also enhanced antibody performance of fucose free glycoforms (Forthal et al., 2010; Zeitlin et al., 2011).

β1,4- galactosylation of the glycan branches is not only important for further sialylation (Castilho and Steinkellner, 2012), but also for mimicking some occurring human-like complex glycan structures that promote effector function and correct protein folding (Bakker et al., 2001).

For this, initial efforts in over-expressing human GalT in plants proved that sub-cellular targeting of the protein is important to avoid competing for substrate with glycosylation enzymes that act earlier in the *N*-glycosylation process (Palacpac et al., 1999; Bakker et al., 2006; Strasser et al., 2009; Vezina et al., 2009).

Glycosyltransferases are type II transmembrane proteins consisting of an amino terminal cytoplasmic tail, a signal anchor transmembrane domain, a stem region (CTS region), and a luminal catalytic domain. The CTS region is responsible for the sub-Golgi targeting of a glycosyltransferase. The enzyme localisation controls the type of oligosaccharides attached to the protein and therefore regulates the final glycosylation pattern, making sub-Golgi targeting important for *N*-glycan modification, as it has been previously stated (Schoberer et al., 2014).

Using the ΔXF platform, a modified version of human β1,4-GalT was overexpressed, but where the endogenous CTS domain was replaced by rat α2,6-sialyltransferase CTS domain, which targets the protein to the late Golgi (figure 3) (Strasser et al., 2009). Analysis of glycan structures attached to anti-HIV mAbs expressed in this plant platform displayed a predominant digalactosilated structure, with improved functional activity.

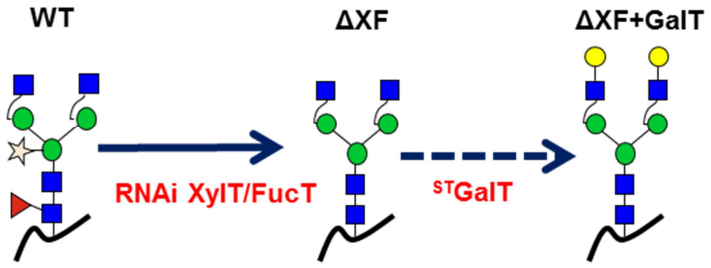

Figure 3: Outline of the glycoengineering in *N.bethamiana* to allow synthesis of fully galactosylated glycans. The ΔXF line was obtained using RNAi technology and later galactosylation of terminal GlcNAc by expressing a modified version of the human β1,4-galactosyltransferase.

Sialylation is an additional challenge, as plants do not possess the mechanism to produce, transport or use the Neu5Ac need for sialylation (Castilho and Steinkellner, 2012). Mammal cell cultures, like CHO, are able to sialylate proteins, but in a different linkage than the humans (Castilho and Steinkellner, 2012). Since some proteins need the properly sialylated glycoform, the versatility of plants was employed. Therefore, in order to achieve

sialylation, apart from GalT and ST, the genes for the production and transportation of sialic acid to the Golgi apparatus must also be expressed.

This was achieved by co-expressing six genes from the mammalian sialic acid pathway (figure 4) (Castilho et al., 2010). These genes allowed the production, transport and transfer of sialic acid to recombinant proteins. This was initially shown for anti-HIV mAb carrying mono and di-sialylated glycans.

In the same way, sialylation was achieved in other pharmaceutically relevant proteins (Castilho et al., 2013; Jez et al., 2013; Castilho et al., 2014; Loos et al., 2014; Schneider et al., 2014a; Castilho et al., 2015).

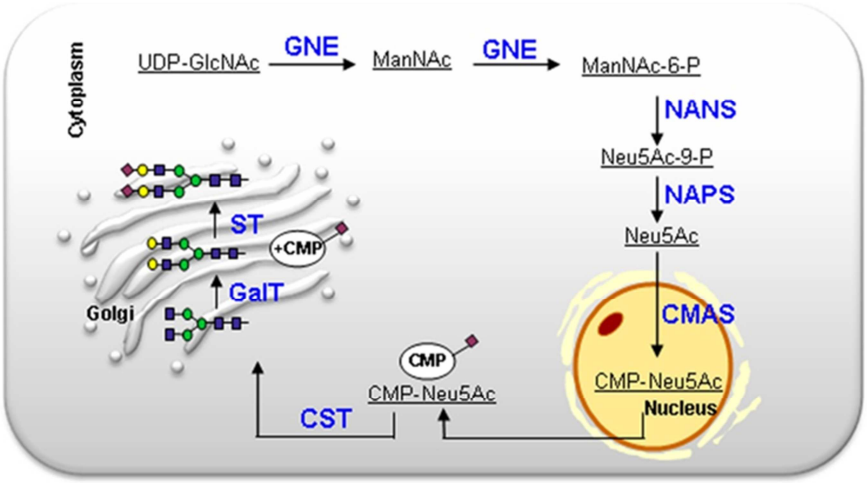

Figure 4: Sialic acid pathway in mammals. The genes expressed in plants for achieving sialylation were: GNE, UDP-*N*-acetylglucosamine2-epimerase/*N*-acetylmannosamine-kinase; NANS, UDP-N-acetylglucosamine 2-epimerase/N-acetylmannosamine-kinase; CMAS, CMP-Neu5Ac synthetase; CST, CMP-Neu5Ac transporter; GalT, β1,4-galactosyltransferase; ST, α2,6-or α2,3-sialyltransferase. Adapted from (Castilho et al., 2010).

1.2.2 Hexosaminidase activity in plants

Another major glycoform of plant produced proteins is $MMXF^3$, or paucimannosidic structures (Castilho and Steinkellner, 2012). This form does not possess terminal GlcNAc attached to its branches. The reason why some proteins are decorated with this form instead of a complex $GnGnXF^3$ are still not well explained, but the secretory pathway, final destination and intrinsic characteristics of the protein have an influence over the glycosylation pattern.

For instance, while most mAbs or erythropoietin expressed in plants present a $GnGn/GnGnXF^3$ glycoform (Strasser et al., 2008; Castilho et al., 2011a; Castilho et al., 2011b), follicle stimulant hormone (Dirnberger et al., 2001), human lactoferrin (Samyn-Petit et al., 2003) and alpha-1 anti-trypsin (Castilho et al., 2014) display MMX or $MMXF^3$ glycoforms.

The presence of xylose and fucose in these paucimannosidic structures indicates that the proteins were processed through the Golgi apparatus, and the reduction in the glycans

happens later, during the storage or secretion of the protein (Castilho and Steinkellner, 2012).

Paucimannosidic structures usually are usually observed in vacuole-stored proteins, but also to some extent in proteins secreted to the apoplast (Liebminger et al., 2011) and their truncation is caused by β-*N*-acetylhexosaminidases. This can affect the function and the immunogenic character of produced proteins, since mammals do not produce such structures (Liebminger et al., 2011).

Two major enzymes are responsible for this phenomenon. HEXO1, located in the vacuole, and HEXO3, present in the plasma membrane and the apoplast (Strasser et al., 2007). Both display the capacity to reduce complex glycans to paucimannosidic structures, and their different locations indicates that they act over distinct glycoproteins (Liebminger et al., 2011).

It is then important to identify which of the hexosaminidases acts over the secretory pathway. If a protein is targeted for secretion, and displays paucimannosidic glycans, it is likely that such glycan is caused by the activity of HEXO3. This fact was proved by gene knockout in *A. thaliana* (figure 5)(Castilho et al., 2014).

Using the available *A. thaliana* individual-knockout of HEXO1 and HEXO 3 to express A1AT (signalled for secretion) it was observed through LC-ESI-MS that a knockout of HEXO1 still produced paucimannosidic structures while the knockout of the HEXO3 restored the A1AT attached glycans to the regular $GnGnXF^3$ profile.

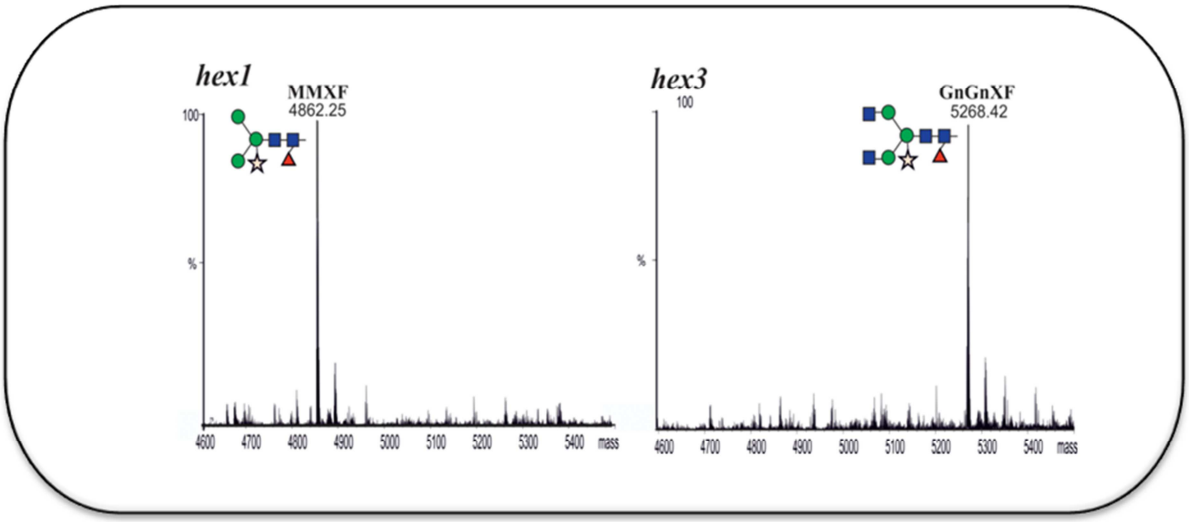

Figure 5: LC-ESI-MS spectra of A1AT expressed in *A.thaliana* HEXO1 knockout line (*hex 1*) and HEXO3 (hex3) knockout line. Adapted from (Castilho et al., 2014).

1.3 Transient expression in plants

What is arguably the greatest advantage of plant produced recombinant proteins is the capacity of plants to express desired genes transiently, leading to the flexibility of the platform.

Transiently transfected cells express the target gene but do not integrate it into their genome. These cells express the transiently transfected gene for a finite period of time, usually several days, after which the foreign gene is lost.

Transient expression technology has been improved and optimised along the years.

Nowadays the technique routinely uses a combination of viral based vectors with agroinfiltration. One example of this technology is magnifection using the magnICON® vectors, developed by Icon Genetics (Halle, Germany). The bacteria are delivered into leaves by vacuum infiltration, and once T-DNA is transferred to the plant cell nucleus the viral machinery takes over allowing massive RNA and protein production (Gleba et al., 2014).. Among the most often used viral backbones are those of the RNA virus Tobacco mosaic virus (TMV) and Potato virus X (PVX), as seen in figure 6.

The TMV based vector possesses a viral particle without the coat protein (figure 6). This way, the viral particle can move through the tissue of the infected plant organ (due to the existence of a movement protein), but not through the vascular system. The viral particle is additionally modified by the removal of splice sites, addition of plant introns and changes in the codon usage ensures that the processing of this DNA by plants is successful in more than 90% of the cells (Gleba et al., 2007).

These modifications enable the control of the infected area and the improvement of recombinant protein size and yield (Gleba et al., 2007).

Other viral particles, like PVX, do not need such a modification and can still be used effectively (Gleba et al., 2014)

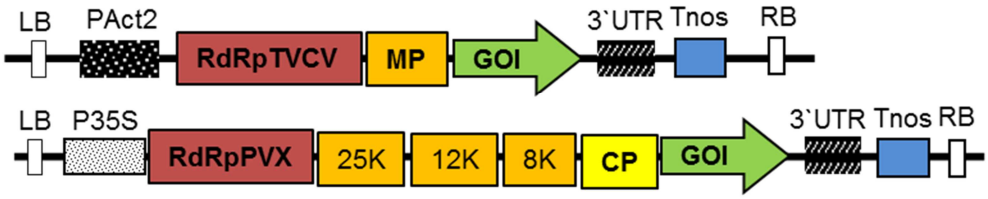

Figure 6: Schematic representation of magnICON vectors. The modified TMV-based and PVX-based magICON vectors with a targeting sequence for the secretory pathway can be used simultaneously to express an antibody's heavy and light chain. 25K, 12K and 8K: 25kDa, 12kDa and 8kDa triple gene block of PVX movement proteins; 3'UTR: TMV or PVX 3'-untranslated region; CP: coat protein;GOI: gene of interest; LB: left border; MP: movement protein from TMV; P35S: cauliflower mosaic virus 35S gene promoter; PAct2: *Arabidopsis* actin 2 promoter; RB: right border; RdRpPVX: RNA-dependent RNA polymerase from potato virus X; RdRpTVCV: Turnip vein clearing virus RNA-dependent RNA polymerase.

If more than one polypeptide needs to be expressed in the same cell such as is the case for the expression of antibodies, using the same virus as base for the replicons will not succeed, as there is no co-expression of both in one cell (Giritch et al., 2006). In such cases vectors are built from the backbones of two different noncompeting viruses, e.g. TMV and PVX, where the co-expression level is able to reach 95% of the cells (Giritch et al., 2006). Several antibodies and vaccine antigens produced by magnifection are currently in clinical trials (Gleba et al., 2014).

1.4 Recombinant proteins: Antibodies

Antibodies, part of the immunoglobulin superfamily, are some of the most sought after biopharmaceuticals in the world, heading the industry's annual production and sales. They are part of the immune system and bind to foreign objects, called antigens. These can be, among many others, bacteria, viruses or tumours. By binding to antigens, antibodies target them for deletion or exert an effector function. Sometimes, antibodies can bind to the bodies' own objects, causing auto-immune diseases.

Antibodies are usually a Y-shaped molecule, with two heavy chains and two light chains (figure 7). They possess a Fc region which encompasses the constant region of the heavy chains. It is this region that will bind to cell receptors or complement proteins responsible for defence mechanisms like cell lysis. The binding to the antigen is made by the fragment antigen-binding (Fab region).

There are five types of antibodies (IgA, IgD, IgE, IgG, IgM), depending on the constant region of the heavy chain. This region is very conserved and homogenous in each type. On the other hand, the variable region is very flexible, so it can bind to different epitopes.

As other proteins, antibodies are also glycoproteins. The glycosylation sites (number and type of glycosylation) will also be different according to the type of Ig in question.

If an antibody batch is produced from one single parental cell line, these molecules will be called mAbs, or monoclonal antibodies, and are identical (which is of the utmost interest for homogenous protein production).

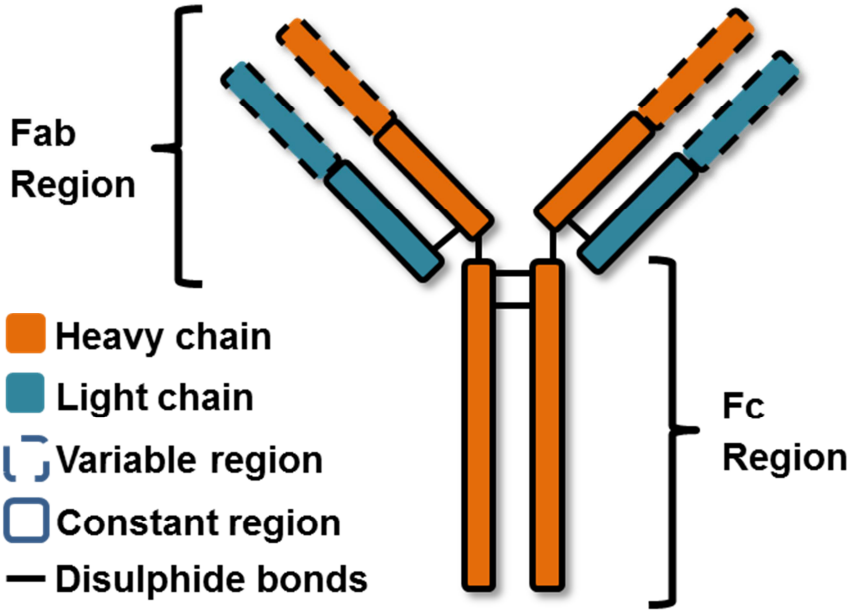

Figure 7: General antibody structure. Bonds established between heavy chains are disulphide bonds, as well as those between heavy and light chain.

1.4.1 Rituximab

Rituximab is a monoclonal IgG antibody, with one complex *N*-glycosylation site (figure 8) on the asparagine 297 residue (Dimitrov et al., 2007). The whole molecule has a molecular weight of 145 kDa, but differences in glycosylation patterns will slightly change this value.

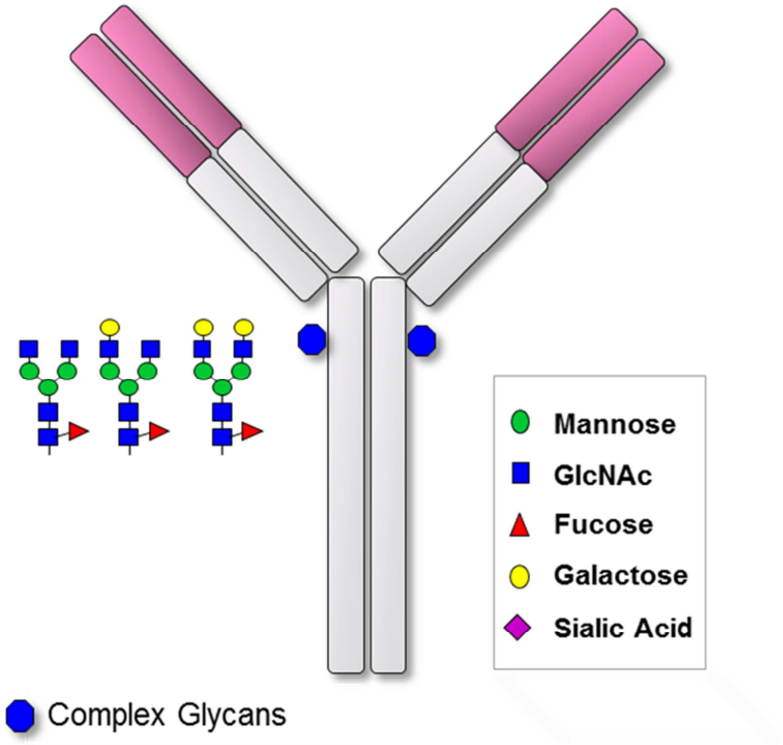

Figure 8: Basic IgG structure with common glycans usually found on the Asn 297 residue. The fucose found in this glycans corresponds to the α1,6 linkage.

It is a chimeric antibody (constant fraction is human, variable fraction is from mouse) commercially used for the treatment of non-Hodgkins lymphoma, other B-cell related malignancies and auto-immune diseases. It binds to CD20 receptors on the surface of these cells (Rudnicka et al., 2013).

The monosaccharide content of the complex glycans in monoclonal IgGs (mAbs) is highly variable. More than 30 different glycoforms linked to Fc have been described (Burton and Dwek, 2006)

The function of this antibody, like other IgGs, is influenced by glycosylation patterns (see review in (Stoger et al., 2014)).

The impact of the carbohydrate structure on the biological functions of IgGs remains unresolved. Several studies have investigated the influence of the glycan composition on the effector functions of IgG.

It has been demonstrated that the Rituximab effector activity depends strongly on the content of fucose in the glycan structure (Kanda et al., 2007). Thus, it is important that for correct activity, the glycan structure should be engineered. For instance, the insertion of bisecting GlcNAc decreases core fucosylation, which enhances antibody-dependent cell cytotoxicity effects, while galactosylated forms contribute to correct activation of the complement system (Zauner et al., 2013).

It has been suggested that for IgGs, another possible function is to mediate anti-inflammatory responses (Anthony and Ravetch, 2010). In fact, α2,6-linked sialylated glycans in IgG have been proven to cause anti-inflammatory effects on mice (Kaneko et al., 2006), but further studies are still needed.

Earlier data indicated that avoiding Fc glycan sialylation can offer another means of optimizing ADCC activity of Abs (Kaneko et al., 2006; Scallon et al., 2007). However in these previous studies mAbs were produced differing in levels of α2,3-terminal sialic acid and it was not clear whether both 2,6- and 2,3-sialylated antibodies would have a similar effect on cytotoxicity. Recently it was found that the effect of di-sialylated N-glycan on activity depends on the linkage. Affinity studies revealed that α2,6-sialylated Rituximab has a stronger interaction with FcγRIIIa, whereas a detrimental effect was observed with the α2,3-sialylated Rituximab. Indeed, two terminal α-2,6-linked sialic acids (NaNa) constitutes a common and optimized structure for the enhancement of antibody-dependent cell-mediated cytotoxicity, complement-dependent cytotoxicity, and anti-inflammatory activities (Lin et al., 2015).

It is therefore of the most importance to verify if sialylated patterns are suitable for the production of anti-inflammatory biopharmaceuticals, as well as testing the effects of other glycan structures for the same purpose. Rituximab was selected as a model for this

investigation because it has been used for the treatment of both cancer and autoimmune diseases.

Rituximab ranks among the top 10 biological drugs in Europe. In 2011 iBio, working on the plant-made pharmaceutical, announced the production of rituximab in non-transgenic green plants. The expression of rituximab in plants resulted in a self-assembled antibody structure. Testing showed that plant-produced rituximab was able to demonstrate the same antigen recognition and target cell cytotoxicity observed with rituximab manufactured in mammalian cells.

1.4.2 KBPA

IgM antibodies have several favourable properties that support their use as therapeutic tools: their pentameric form provides 10 antigen binding sites, they bind antigens with high avidity, and IgM antibodies are very effective complement activators (Spiegelberg, 1989).

IgM monomers consist of two light and two heavy chains. The heavy chains of most antibodies (such as IgG) contain three constant domains, whereas the heavy chains of IgM have four (giving them a molecular weight of 72 kDa instead of 55 kDa). It has five *N*-glycosylation sites (figure 9; Asn 171, 332, 395,402 and 563) and 95% of the antibodies associate in a pentameric structure, assembled by a joining chain (figure 10). Pentameric IgM is an important component of the first line of defense against foreign pathogens (Boes et al., 1998).

KBPA is a human monoclonal antibody, of the immunoglobulin M class. This antibody reacts to the O-polysaccharide moiety of *Pseudomonas aeruginosa* (Lazar et al., 2009), responsible for multiple kinds of infections.

Altogether, IgM structure is about 950 kDa (Loos et al., 2014), a hexameric structure is also possible, though.

Such a complex structure means that IgMs are possibly the most difficult antibodies for plants to produce, due to size and expression coordination of genes (apart from heavy chain and light chain genes, two additional genes must be expressed, for the joining chain and for a chaperone which allows for secretion) (Loos et al., 2014).

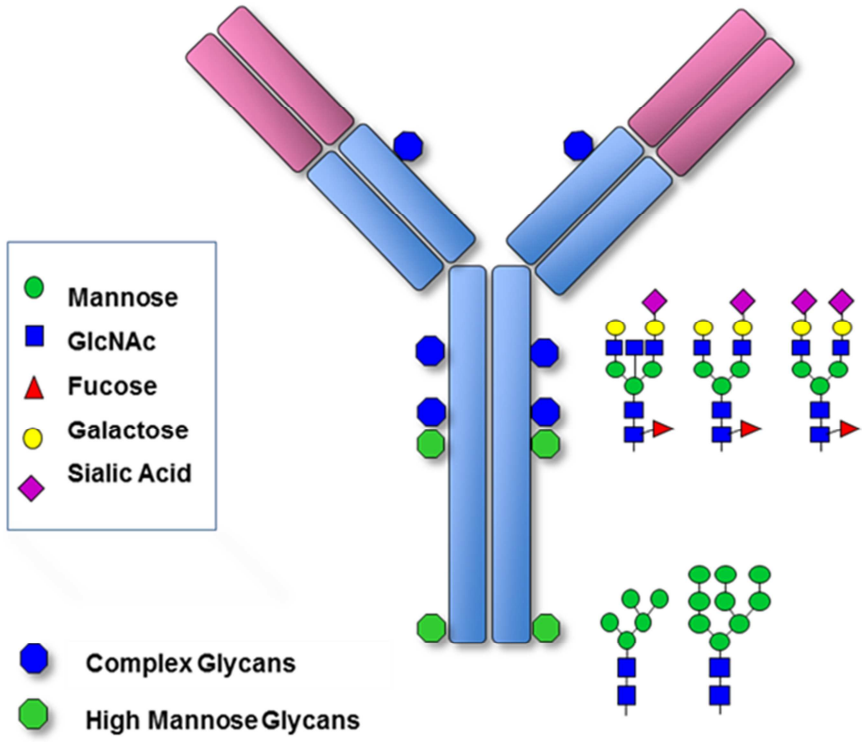

Figure 9: IgM monomer structure with *N*-glycosylation sites and typical glycans.

While it is known that the pentameric/hexameric structure of IgM antibodies is important for the correct activity, the glycosylation patterns are still poorly studied and need further elucidation as to their influence (Loos et al., 2014). Even so, it is believed that like other Ig types, they exert influence over the activity of the antibody.

Recently the report on site-specific N-glycosylation pattern of human serum IgM showed the presence of oligomannosidic glycans in three sites (Asn171, 402 and 563) although major glycoform on Asn171 were complex mono-sialylated fucosylated glycans. In Asn 332 and 395 only complex-type glycans with one or two sialyic acid residues and bisected GlcNAc were detected (Pabst et al., 2015).

The first and only report of plant made IgM antibodies (Loos et al., 2014) demonstrated assembly of both pentameric and hexameric structures in *Nicotiana benthamiana*. Plant-derived SM6 IgM exhibited complex and oligomannosidic N-glycans in a site-specific manner as in human-serum IgM. Moreover the biological activity of plant-derived SM6 was comparable to the human-cell-derived counterparts. Glycoengineering allowed the generation of SM6 decorated with mono- and di-sialylated glycans (~33%).

Unfortunately, the data on IgM glycoengineering and the impact of glycoslytion on IgM activity is still scarce when searching the available literature. This means not much more that the work of Loos and co-workers could be used as reference for the present study.

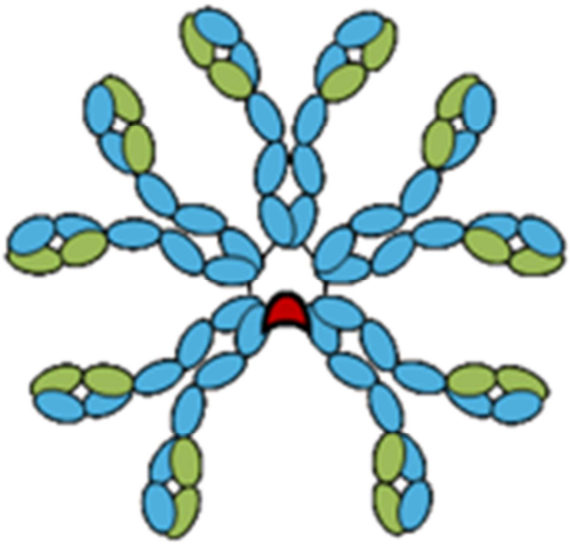

Figure 10: Typical pentameric IgM structure. The complex protein is formed by 10 heavy chains (blue), 10 light chains (green) and a joining chain (red) which allows for the formation of the polymeric structure.

1.5 Protein purification

While upscaling and expression of proteins are processes with big potential in plant platforms, purification is a possible problem. This is because purification is aimed for the product, not the platform, and because plants have contaminants that can make this process more complex and costly (RuBisCO, for instance) (Stoger et al., 2014).

In fact, the upstream technological achievements have not been matched by downstream processing advancements. Extraction conditions have been optimized for numerous proteins on a case-by-case basis leading to the development of platform-dependent approaches. Non-chromatographic purification methods, such as aqueous two-phase partitioning and membrane filtration, have been evaluated as low-cost purification alternatives. Strategies for the primary recovery and purification of recombinant proteins, comparing the process economics between systems, were recently reviewed (Wilken and Nikolov, 2012).

Methods of purification vary from protein to protein, making it impossible to design a general purification strategy valid for all cases. Ideally, methods should allow rapid isolation of proteins from plant material achieving a high degree of purity. Tandem Affinity Purification (TAP) uses affinity tags meaning polypeptides or small proteins fused to the protein of interest and allow purification via an affinity matrix. A wide variety of affinity tags is currently available. The ideal tag is small and allows rapid and flexible purification from a complex mixture, achieving high yield and purity. A small tag is generally less likely to interfere with the biological function of a protein.

Another possible solution lies in specific affinity chromatography. The use of resinous substances containing proteins that bind to regions of the desired product may separate the recombinant products from the rest of the plant cell pollutants. Afterwards, precipitation by pH shift releases the product from the protein in the resin.

There is, however, a concern if the purified product will maintain functionality after purification.

The main classes of serum immunoglobulins (e.g., IgG, IgM) share the same general structure, including overall amino acid composition and solubility characteristics.

The most widely used affinity chromatography purification step in industry today is the capture of antibodies using Protein A ligand. Protein A is a bacterial protein from *Staphylococcus aureus*, with the capacity to bind mammalian antibodies of class immunoglobulin G (IgG) with high affinity (Forsgren and Sjoquist, 1966). The gene for Protein A has been cloned and expressed in *E.coli* allowing for the production of large quantities of recombinant Protein A.

The affinity chromatography method has been proven successful for both IgG and IgM antibodies.

Plants as expression platform are still a relatively new process, and purification methods can still have room for improvement.

1.6 Aims

The aims of this work were to set up and optimise the upscaling production of plant-derived IgG and IgM antibodies within laboratory facilities. For this Rituximab and KBPA were used as models for IgG and IgM, respectively. The plant host was the *N.benthamiana* glycosylation mutant and glycogenes were transiently expressed to simultaneously modulate the glycosylation profile of the recombinant IgG and IgM. Rituximab was produced with different attached glycans in order to test the influence of these structures over the anti-inflammatory activity of IgGs. For KBPA the aim was to study the contribution of sugar moieties to the function of IgMs, which is yet unknown.

The second part of this project deals with the presence of paucimannosidic glycans in plant-produced recombinant proteins.

The preliminary and encouraging results on HEXO3 knockouts in *Arabidopsis thaliana* led us to pursue the downregulation of hexosaminidases in *N. benthamiana*.

A1AT was used as quality control for this part of the investigation. Ultimately we aim at the genetic transformation of plants with our construct and produce a new plant expression platform unable to decorate recombinant proteins with paucimannosidic glycans.

2 Materials and Methods

2.1 Materials

2.1.1 Buffers and Solutions

Solutions and buffers in this work were prepared with ultrapure water (18 M Ω cm at 25℃) and analytical grade reagents. If not stated otherwise, reagents were acquired from the following companies: Fluka, Gibco BRL, Merck, Roth, Sigma-Aldrich, VWR.

Coomassie staining solution:

- 0.5 % (w/v) coomassie brilliant blue G250
- 50 % (v/v) methanol
- 7 % (v/v) acetic acid

Coomassie destaining solution:

- 20 % (v/v) methanol
- 7 % (acetic acid)

Ethidium bromide:

- Stock solution: 10mg/L in dH_2O at +4℃
- Working solution: 600 ng/µL in dH_2O at +4℃

Protein A elution buffer:

- 100 mM glycine.HCl pH 2.5

IgM capture select elution buffer:

- 100 mM glycine.HCl pH 2.2

Protein extraction buffer pH 6.8:

- 500 mM NaCl
- 100 mM Tris.HCl
- 40 mM (L+) ascorbic acid

PBS (phosphate buffered saline) 10 X:

- 1.4 M NaCl
- 27 mM KCl
- 10 mM Na_2HPO_4
- 2 mM KH_2HPO_4

PBS 1 X pH 7.34/8.0/6.0:

- 1:10 PBS 10 X in dH_2O, corrected to target pH with either HCl or NaOH

Infiltration buffer:

- 10 mM MES, pH 5.6
- 10 mM $MgSO_4$
- 1:10000 Acetosyringone

SDS-PAGE running buffer 10 X:

- 0.25 M Tris
- 1.92 M glycine
- 1 % SDS

SDS-PAGE running buffer 1 X:

- 1:10 SDS-PAGE running buffer 10 X in dH_2O

SDS-PAGE sample buffer 3 X:

- 250 mM Tris.HCl, pH 6.8
- 40 % glycerol
- 8 % SDS
- 20 % mercaptoethanol
- 0.2 % bromophenol blue

TAE (Tris-acetate-EDTA) 50 X pH 8.0:

- 2 M Tris
- 1 M acetic acid
- 0.05 M $Na_2EDTA*2H_2O$

TAE (Tris-acetate-EDTA) 1 X:

- 1:50 TAE 50 X in dH_2O

2.1.2 Enzymes

Restriction enzymes and proper buffers obtained from either New England Biolabs or Thermo Scientific.

- *AscI* (10 U/µL, #R05585)
- I-*SceI* (10 U/µL, #ER1771)
- *KpnI*-HF (20 U/µL, #R3142S)
- *BglII* (20 U/µL, #R0144S)
- *BamHI*-HF (20 U/µL, #R3136S)
- *XhoI* (20 U/µL, #R01465)
- *EcoRV* (10 U/µL, #ER0301)

Other enzymes used:

- Antartic Phosphatase (5 U/µL) with 10x buffer (New England Biolabs, #M0289S)
- Phusion® High Fidelity DNA Polymerase (2 U/µL) with 5x GC buffer (New England Biolabs, # M0530S).
- GoTaq® G2 DNA Polymerase (5 U/µL) with 5x Green GoTaq® Buffer (Promega, # M7845)
- T4 DNA Ligase (100 U/µL) with 10x Ligase Buffer (Promega, # M1801)

- Sequencing Grade Modified Trypsin (100ng/µL in buffer) (Promega # V511A)

2.1.3 Protein and DNA markers/Loading dye

Markers and loading dye were obtained from Thermo Scientifc.

- 6x DNA Loading Dye
- GeneRuler™ 1 kb DNA Ladder (#SM0311)
- GeneRuler™ 100 bp Plus DNA Ladder (#SM0321)
- PageRuler™ Prestained Protein Ladder (#26616)

2.1.4 Media

Prepared media were autoclaved and then stored at +4℃.

Lysogeny Broth (LB)

- 5 g/L yeast extract
- 10 g/L tryptone/peptone
- 5 g/L sodium chloride

LB agar

- 5 g/L yeast extract
- 10 g/L tryptone/peptone
- 5 g/L sodium chloride
- 15 g/L agar

Super Optimal broth for Catabolite repression (SOC), pH 7.0

- 2 % (w/v) bacto-tryptone
- 0.5 % (w/v) yeast extract
- 10 mM NaCl
- 2.5 mM KCl
- 10 mM MgCl2
- 10 mM MgSO4
- 20 mM D(+)-glucose monohydrate

2.1.5 Antibiotics

Ampicillin

- Stock solution: 100 mg/mL (in dH_20)
- Working solution: 100 µg/mL (= 1:1000 diluted stock solution)

Gentamycin

- Stock solution: 25 mg/mL (in dH_20)

- Working solution: 12.5 µg/mL (=1:2000 diluted stock solution)

Kanamycin

- Stock solution: 50 mg/mL (in dH_20)
- Working solution: 50 µg/mL (= 1:1000 diluted stock solution)

Spectinomycin

- Stock solution: 100 mg/mL (in dH_20)
- Working solution: 140 µg/mL (= 1:700 diluted stock solution)

2.1.6 Kits

- Wizard® Plus Minipreps DNA Purification System (Promega, Madison, MO, USA # 75964)
- Invisorb MSB® Spin PCRapace (Invitek, Berlin, Germany #1020110400)
- FavorPrep® Gel/PCR purification kit (Favorgen #FAGCK001)

2.1.7 Bacterial Strains

- Electrocompetent *Escherichia coli* DH5α
- Electrocompetent *Agrobacterium tumefaciens* UIA143

2.1.8 Plants

- *Nicotiana benthamiana* mutant plant line ΔXF lacking α1,3-fucose and β1,2-xylose glycosylation modifications (Strasser et al., 2008)
- *Nicotiana benthamiana* mutant plant line Ce144 lacking α1,3-fucose/β1,2-xylose glycosylation and with stable transformed Ce144 construct for the production of 5-acetylneuraminic acid (Loos and Castilho, 2015)
- *Nicotiana benthamiana* wild type plants.

2.1.9 Constructs and vectors

Peptide/DNA sequence of recombinant proteins can be found in the annex section, along with the scheme of the constructs.

Rituximab (http://www.imgt.org/mAb-DB/mAbcard?AbId=161)

- A2TMVRxHC - Heavy chain of Rituximab antibody (Acc. No. AX556949)
- A2PVXRxLC - Light chain of Rituximab antibody (Acc. No. AX556921)

KBPA (http://www.imgt.org/mAb-DB/mAbcard?AbId=243)

- A2TMVKBPAHC - Heavy chain of KBPA antibody
- A2PVXKBPALC - Light chain of KBPA antibody

- pPT2M-J-Chain - Joining chain for KBPA antibody polymerisation
- ERp44 - Chaperone for correct assembly of polymeric structures

A1AT (Accession:AAB59375.1)

- p27A1AT - A1AT protein construct

Cloning vectors

- SAT1: pSAT family of plasmids (GenBank Accession No. DQ005461) with a multiple cloning site between the octopine synthase promoter and terminator flanked by AscI restriction sites (Chung et al., 2005).
- SAT4: pSAT family of plasmids (GenBank Accession No. DQ005466) with a multiple cloning site between the 35S promoter and terminator flanked by I-Sce restriction sites (Chung et al., 2005)
- RCS: pPZP-RCS2 binary vector (GenBank AccessionNo. DQ005454) with a cassette for *EPSP* synthase (3-phosphoshikimate 1-carboxyvinyltransferase) expression conferring glyphosate *resistance*. Vector contains restriction sites for assemble of several pSAT expression cassettes.

Glycosylation constructs

- GnTII: *A. thaliana* α1,6-mannosyl-β1,2-N-acetylglucosaminyltransferase II
- GNE: mouse UDP-N-acetylglucosamine 2-epimerase/N-acetylmannosamine-kinase
- NANS: human N-acetylneuraminic acid phosphate-synthase
- CMAS: human CMP-N-acetylneuraminic acid synthase
- CST: mouse CMP-sialic acid transporter
- STGALT: human β1,4-galactosyltransferase
- ST: rat α2,6-sialyltransferase
- FUT11: A. thaliana α1,3-fucosyltransferase
- pC144 - Multi gene vector carrying GNE, NANS and CMAS expression cassettes for sialic acid production
- pG371 - Multi gene vector carrying CST, STGALT and ST expression cassettes for galactosylation, transport and transfer of sialic acid for sialylation

Hexosaminidase constructs

- pMA-TNbHexo3: plasmid containing the synthetic sequence of the intron 2 (XTI2) sequence from the Arabidopsis β1,2-xylosyltransferase and the antisence of a 235 bp fragment from the N. benthamiana hexosaminidase 3 (obtained from Ao. Prof. Dr. Richard Strasser of the department of applied genetics and cell biology of the University of Natural Resources and Life Sciences, Vienna)

- Hexo3RNAi: *N. benthamiana* hexosaminidase 3 RNAi construct in SAT4 assembled in RCS binary vector
- Hexo3/1RNAi: *N. benthamiana* hexosaminidase 3 RNAi construct in SAT4 and *N. benthamiana* hexosaminidase 1 RNAi construct in SAT1 assembled in RCS binary vector
- p31Nbhexo3: *N. benthamiana* hexosaminidase 3 construct fused to mRFP (kindly supplied by Richard Strasser)

2.1.10 Primers

5'-3' sequences of primers are displayed. Products were obtained from Sigma-Aldrich. Sequences are as follows:

- Nb-CAT1 - CATTCGCGGTTTTGCTGTC
- Nb-CAT2 -TGGTGGCGTGGCTATGATTTGTA
- Nb-hexo3 F2 - ATTTAGTATAGTGATGGGGAAGTTAGGATT
- Nb-hexo3 R2 - ACGTAACTATTGCTGATAGCAAGAACCTGGATC
- Nb-hexo1 F4 - TATAACTAGTATGTCCTCAAATTCCCAATGTCTT
- Nb-hexo1 R4 - TATAGGATCCTTGTTCATAGCATGATCCTGGGC
- Nb-hexo3 R5 - ATGTTCATTGCTCTTCGTCACC
- EPSPS F3 - GACGTCGCATTGGTACGG
- RCS2 F2 - CTCTCTTAAGGTAGC
- SAT1 F1 - GGTGTGGCCTCAAGGATAATCGC
- SAT1 R1 - CATGCGATCATAGGCGTCTCGC
- SAT4 F1 - CATTCTACTTCTATTGCAGC
- SAT4 R1 - GAACTACTCACACATTATTCTG
- sshexo3 F1 - TATACTCGAGGCAAAAACAGTTTATGG
- sshexo1 F1 – TATACTCGAGATTGTTCATTCCGATAAC

2.2 Methods

2.2.1 Basic procedures

Bacterial cultures - Electrocompetent or already transformed *E. coli* and *A. tumefaciens* cells were kept in stocks of 1mL LB and 1mL 100% glycerol at -80℃.

For infiltration, 100 µL of agrobacterial cultures were incubated overnight in 50 mL LB with the appropriate antibiotic concentration. Cell cultures were incubated overnight (~20 h) at 29℃ shaking (180 rpm).

For plasmid purification, a single *E. coli* colony growing in agar plates was inoculated in 5 mL LB and grown overnight at 37℃.

LB agar plating - LB agar media was microwaved until liquid. Afterwards, it was left to cool to 50-60℃, inoculated with the appropriate antibiotic and plated onto 9 cm diameter plastic petri dishes.

OD_{600} measuring - Bacterial concentration was determined by measuring the optical density at 600 nm (1.0 OD_{600} equals $5x10^8$ cells) with BIO-RAD Smart-Spec ™ 3000 photometer. Cells grown in LB media overnight were centrifuged and resuspended in 35 mL infiltration buffer before measuring.

Agarose gel electrophoresis - 1 % (w/v) agarose gels were used for separation of DNA fragments. One gram agarose was dissolved in 100 mL 1x TAE buffer in the microwave oven for about 2 minutes. After cooling down, 100 µL ethidium bromide working solution was added and the gel was casted into the gel casting chamber with fitted combs.

2.2.2 Molecular biology methodology

PCR (polymerase chain reaction) - PCR was used to amplify copies of a DNA fragment from just a few to thousands or millions of copies.

It consists of temperature cycles, repeated dozens of times. These comprise a denaturation period, an annealing period and an elongation period, which allow for a DNA molecule to denature, connect to a primer and be reproduced by a DNA polymerase.

Additionally to the temperature cycles, there is one first step of denaturing and one last step of elongation.

For a PCR, the needed components include DNA template, forward and reverse primers (DNA template complementary sequences), a thermos stable DNA polymerase, a mix of nucleotides for the elongation of new DNA chains (100 mM dNTPs, or deoxynucleotide triphosphate), a buffer that provides optimal pH and cation concentration for the polymerase and DMSO, which facilitates the annealing phase.

All the reactions were performed in an Applied Biosystems Thermal Cycler 2720.

Settings for PCR - Settings were different according to the applications of the PCR (tables 1 and 2).

Briefly, the two main uses of PCR were colony screening or DNA fragment cloning. The main differences are the DNA polymerase used (Phusion® polymerase was used for cloning since it has a 3'-5' proofreading ability), the temperature of annealing and the total reaction

volume. The DNA template, in case of colony screening, was a colony suspended in 10 µL dH_2O and microwaved for 1 minute.

Table 1: PCR conditions for gene cloning.

Reagent	Volume (µL)
5x Phusion Buffer	20
dNTPs	2
DMSO	5
Primer Forward	2
Primer Reverse	2
Template	1.5
Phusion	1.25
dH2O	66.25
Final Volume	100

Phase	Temperature (℃)	Time	Cycles
Initiation	95	5 min	1
Denaturing	95	45 s	25
Annealing	53	45 s	
Elongation	72	1 min	
Extension	72	5 min	1
Hold	14	∞	

Table 2: PCR conditions for colony screening.

Reagent	Volume (µL)
5x GoTaq Buffer	5
dNTPs	0.5
DMSO	1.25
Primer Forward	0.5
Primer Reverse	0.5
Template	10
GoTaq	0.25
dH2O	7
Final Volume	25

Phase	Temperature (℃)	Time	Cycles
Initiation	95	5 min	1
Denaturing	95	50 s	25
Annealing	55	50 s	
Elongation	72	1 min	
Extension	72	5 min	1
Hold	14	∞	

Plasmid purification - This procedure was done with the Wizard® Plus Minipreps DNA Purification System kit, following its instructions. To harvest cells, 5 mL of overnight culture were centrifuged at 10.000 rpm for five minutes (RT). Afterwards, cells were resuspended in 250 µL of Cell Resuspension Solution and mixed with the same volume of Cell Lysis Solution. 10 µL of Alkaline Protease Solution was added to the resuspended cells and incubated for 5 minutes at room temperature, and after that 350 µL of Neutralization solution was added. The solution was again centrifuged at 10.000 rpm for ten minutes (RT). The clear supernatant was decanted into given Spin Columns, centrifuged at 13.000 rpm for one minute (RT) and washed two times with 750 and 250 µL of Washing Solution (again centrifuged at 13.000 rpm each time, for one minute, RT). The sample was then dried (13.000 rpm, 2 minutes, RT) and eluted in 35 µL of dH_2O at 75℃ (13.000 rpm, one minute). Finally, the purified sample was stored at -20℃.

DNA digestion - For cloning, digestion of vectors and DNA inserts was done. This was achieved by restriction enzymes that either cut the vectors and inserts in a way that the ligation between them is compatible. DNA digestion was also used for testing if cloning was successful.

Information about enzymes, buffers for single or double digestion (With two different restriction enzymes) and incubation conditions were obtained from NEB (www.neb.com) or Thermo Scientific (www.thermoscientific.com) websites.

Digestions were prepared in 1.5 mL Eppendorf tubes and incubated for 1-3 hours at optimal temperature for the enzyme activity (Table 3). DNA digestion was analysed by agarose gel electrophoresis. One µL of digestion mixed with 2 µL 6x Loading dye and 7 µL dH_2O were loaded onto a 1 % agarose gel (100 V, 30 minutes).

Table 3: Conditions for digestion. These conditions are applied for insert, vector and test digestions, respectively. For double digestions, the enzyme and water volumes were adjusted to fit the final volume (volume of water lowered to compensate for the other enzyme added).

Component	Volume (µL)
Insert	21
10 X Buffer	3
Enzyme	3
dH2O	3
Final volume	30

Component	Volume (µL)
Vector	35
10 X Buffer	5
Enzyme	5
dH2O	5
Final volume	50

Component	Volume (µL)
Recombinant	3
10 X Buffer	1
Enzyme	1
dH2O	5
Final volume	10

Dephosphorylation of cloning vectors – Antarctic phosphatase was used for catalysing the removal of 5' phosphate from the open DNA vectors. This stops open vectors from

ligating to each other or closing again before ligation to the inserts. Table 4 describes conditions for dephosphorilation.

Table 4: Conditions for dephosphorylation. Incubation was done for 1h to 1h30 min at 37℃.

Component	Volume (µL)
Vector	50
10 x buffer	6
Enzyme	2
dH_20	2
Final volume	60

Purification of PCR amplified DNA fragments - MSB®Spin PCRapace Kit was used for purification of DNA fragments out of PCR reaction as well as vectors and inserts after enzymatic reactions. 500 and 250 µL of Binding buffer were added to PCR products open vectors and digested inserts, for samples above and below 50 µL, respectively. Samples were vortexed, transferred into supplied Spin Filter and centrifuged (3 minutes, 12.000 rpm, RT). After drying the samples (2 minutes, 12.000 rpm, RT), the DNA was in 40 µL of warm dH_2O (1 minute, 10.000 rpm).

Purification of DNA from agarose gel - DNA fragments were purified from agarose gels with the NucleoSpin®Extract II kit by the manufacturers' instructions. DNA was cut out of agarose eight well gels with a scalpel under UV light. Cut agarose snips were transferred into a 1.5 mL Eppendorf tube and weighed. For 100 mg of gel, 200 µL of NT buffer were added and incubated at 50℃ for 5-10 minutes to melt agarose. The sample was loaded onto supplied NucleoSpin column, centrifuged (1 minute, 11.000 rpm) and washed with 600 µL NT3 buffer (1 minute, 11.000 rpm). The samples were dried (2 minutes, 11.000 rpm) and eluted in 20 µL dH_2O (70℃) (1 minute, 10.000 rpm).

DNA ligation - For ligation, the insert to vector ratio was 1:3. DNA concentrations were estimated by gel electrophoresis. Table 5 summarizes conditions for DNA ligation.

Table 5: Conditions for DNA ligation. The reactions were incubated for one hour at room temperature and later used for transformation on *E. coli*.

Component	Volume (µL)
open vector	1 µL
insert	3 µL
2 x Rapid Ligation buffer	5 µL
T4 DNA ligase	1 µL
total volume	10 µL

Transformation of *E.coli* - Electrocompetent *E. coli* cells (100 µL) were thawed on ice and 5 µL of ligation mixture was added. The electroporation was performed in a precooled electroporation cuvette (1.80 kV) with Micropulser^{TM} (BIO-RAD). Cells were then inoculated into 900 µL of pre-warmed (37℃) SOC-medium in a 1. 5 mL Eppendorf tube and incubated for 1 hour at 37℃, gently shaking.

The bacteria were plated on LB-agar plates containing the antibiotic specific for plasmid resistance (about 100 µL of bacteria per plate). Plates were sealed with Parafilm and incubated for 12-20 hours at 37℃.

The same procedure was used for transformation of *A. tumefaciens*, but 4 µL of plasmid were used for the transformation and bacteria were incubated for 3 hours at 29℃. 10 µL of the bacteria cell suspension were plated on LB-agar plates containing the antibiotic specific for plasmid resistance and Gentamycin specific for agrobacteria selection.

2.2.3 Protein methodology

Total soluble protein extraction - Extraction of total soluble protein (TSP) from *Nicotiana benthamiana* leaves was performed for recombinant protein purification and later analysis of attached glycans. For small scale purification, 350-400 mg of infiltrated leaf sample were harvested into a 2 mL Eppendorf tube with two metal beads and frozen in liquid nitrogen. The samples were ground using a swing mill MM 2000 (Retsch®, Haan, Germany) for 2 minutes at amplitude 30. Ground material was mixed with 600 µL protein extraction buffer and centrifuged (15 minutes, 13.000 rpm, +4℃). The supernatant was collected in a 1.5 mL Eppendorf tube and was used for further analysis.

For large scale, infiltrated leaves were harvested in groups of up to 100 g and frozen in liquid nitrogen. Leaves were then ground with pre-cooled mortar and pestle. The ground leaf tissue was put into a centrifuge plastic bottle, and 2 mL of protein extraction buffer was added per gram of leaf tissue. The samples were then incubated for 30 minutes at +4℃ with rotation. Then, the extract was centrifuged for 20 min (13.500 rpm, 4℃), filtered twice

through folded Miracloth and re-centrifuged at the same conditions. Finally, the extract was filtered with the aid of a vacuum pump through 8-12 µm mesh and then 2-3 µm mesh filters. Samples were then used for further purification or extract analysis.

Protein A purification - The affinity and specific binding of Protein A to the Fc domain of IgG antibody was used to purify Rituximab.

25 µL of rProtein-A Sepharose™ Fast Flow (GE Healthcare, Freiburg, Germany) were washed 4 times with 500 µL cooled (4℃) 1x PBS and incubated with TSP extract for 1h30 min-2h at +4℃ with constant rotation. The sample was centrifuged (3 minutes, 10.000 rpm, +4℃), the supernatant discarded and the Protein-A Sepharose with bound protein was transferred into Micro Bio-Spin™ Chromatography Column (Bio-RAD). After washing column four times with 500 µL 1x PBS, the proteins were eluted with 30 µL Protein A elution buffer and neutralized with 2 µL 0.5 M Tris.HCl pH 8.0.

For SDS-PAGE analysis, 30 µL of purified protein were mixed with 20 µL of Sample buffer and denatured for 5 minutes at 95℃.

Large scale Protein A purification - For large scale Rituximab purification, rProtein-A Sepharose™ Fast Flow (GE Healthcare, Freiburg, Germany) was used. 1.5 mL of Protein A was aliquoted into a Bio-Rad Econo-Column® and washed with 1X PBS pH 8.0 for 15 minutes at 1.8 mL/min by a Peristaltic Pump P-1 (GE Healthcare, Freiburg, Germany). The crude TSP extract was then pumped at the same speed through the column, and a 5 µL sample of the flow through was taken for SDS-PAGE analysis. The column was washed with 1X PBS pH 8.0, 7.3 and 6 in this order, for 15 minutes each at the previous stated speed. A sample of 5 µL washed through solution was taken for SDS-PAGE. Again at the same speed, Protein A elution buffer was flowed through the column and 8 to 9 1-1.5 mL eluates were obtained. Estimated concentration of eluates was measured; the desired eluates were kept, pooled if the same concentration and a small sample was taken from each for quality control SDS-PAGE.

Large scale IgM capture select purification - For large scale KPBA purification, the protocol applied was similar to the Protein A protocol with minor changes. Instead of Protein A, CaptureSelect™ (GE Healthcare) matrix that targets unique domain on the Fc part of IgM was used. Also, IgM capture select elution buffer was applied.

Purified protein dialysis - For large scale purifications, the eluates were dialysed overnight in 1X PBS pH 7.0, and then twice for two hours the next day (all in 2 L of 1 X PBS). Eluates were then quantified.

Recombinant protein quantification - Protein concentration in purified samples was estimated by absorbance measuring at 280 nm with Nanodrop 2000® spectrophotometer (Thermo Scientific).

SDS-PAGE - Discontinuous sodium dodecylsulfate polyacrylamide gel electrophoresis (SDS-PAGE) was performed for protein separation. 12 % separation gel and 4 % stacking gel were prepared as listed in Table 6.

Table 6: Conditions for the preparation of SDS-PAGE gels.

Component	Volume	
	12 % separation gel	4 % stacking gel
AA:Bis 40% (29:1)	3.0 mL	0.5 mL
1.5 M Tris/HCl pH 8.8	2.5 mL	-
0.5 M Tris/HCl pH 6.8	-	1.26 mL
dH_2O	4.35 mL	3.18 mL
10 % SDS	100 µL	50 µL
10 % APS	100 µL	50 µL
TEMED	10 µL	5 µL

After gel casting and polymerization (with 10 well combs), gels were mounted into the electrophoresis apparatus (BIO-RAD). The apparatus was filled with 1X running buffer. Electrophoresis was done at 150 V for 1h to 1h30 minutes until the sample buffer ran out of the gel. Proteins were then stained with Coomassie brilliant blue staining solution.

Coomassie brilliant blue staining - Coomassie staining was done to visualize purified protein for further in gel tryptic-digestion. After SDS-PAGE, the gel was incubated in Coomassie staining solution for 30 minutes and then in Coomassie destaining solution for about 1.5 hours, changing the destaining solution every 20 minutes until the protein bands were clearly visible.

Sample preparation for *N*-glycan analysis - Bands were cut out from the SDS-PAGE gels, cut into small pieces and transferred into 1.5 mL tubes. 50 µL of 50 % acetonitrile were added to the tubes and incubated for 5 min (RT). This process was repeated and then once again with 100 µL of 100 % acetonitrile, but instead of incubated, the tubes were shaken and the liquid discarded. 30 µL of a 0.1M NH_4HCO_3 solution were added and

incubated at room temperature for 5 min. 30 µL of 100% acetonitrile were added and incubated at room temperature for 15 min. The liquid was discarded and the samples were dried in a speed-vac concentrator (Savant) for 15–20 min. 50 µL of 10mM DTT in 0.1M NH_4HCO_3 solution were added to re-swell dried pieces for 5 min, and then samples were at 54 ℃ for 45 min. The liquid was discarded and 50 µL of 55mM iodoacetamid in 0.1M NH_4HCO_3 were added and incubated at room temperature for 30 min in the dark. The liquid was discarded and the samples washed with acetonitrile as described above. After they were dried in the speed-vac, 20 µL of 100 ng/µL trypsin in 25mM NH_4HCO_3 solution diluted 1:6 were added to the samples and kept for 10 min (RT). Then, the gel pieces were submerged entirely in 25mM NH_4HCO_3 overnight at 37° C. 50 µL of 25mM NH_4HCO_3 were added and the samples vigorously shaken for 15 min. 50 µL of 100% acetonitrile were added and again shaken for 15 min. After this, the supernatant was collected in separate tubes, 50 µL of formic acid were added to the gel pieces and they were shaken again for 15 min. The supernatant was collected into the previous used tubes and this step was repeated. The collected supernatant was dried in a speed-vac and delivered to the chemistry department for analysis.

Analysis of *N*-glycans - The analysis was done by the group of Ao. Univ.Prof. Dipl.-Ing. Dr.Nat.Techn. Friedrich Altmann of the biochemistry department of the University of Natural Resources and Life Sciences, Vienna. The method used was liquid-chromatography electron spray ionization mass spectrometry (LC-ESI-MS) (Stadlmann et al., 2008).

2.2.4 Plant Methods

Cultivation - Plants were grown in a growth chamber at 24℃, with 60 % humidity and a photoperiod of 16 hours of light/ 8 hours of darkness.

30-40 sterile *Nicotiana benthamiana* seeds were sown in 9x9x9 cm pots with soil, covered with a plastic lid and allowed to grow for two weeks. Individual plants were then transferred into one pot each, displayed in trays and covered in plastic wrap. Plants were let to grow an additional 2-3 weeks until ready for infiltration. Plants were watered 3 times per week and fertilized on one of those times.

Agroinfiltration – Transformed *A. tumefaciens* cells were harvested from a 25-50 mL overnight culture by centrifugation (4000 rpm, 15 minutes) and resuspended in 35 mL infiltration buffer. OD_{600} was then measured.

For co-expression suspensions were mixed in appropriate volumes to reach optimal OD_{600} in the total infiltration mix (see table 7). The suspensions were infiltrated through the stomata of the lower epidermal leaf surface.

Table 7: Optimal OD for infiltration of each construct

Construct	Infiltration OD	Construct	Infiltration OD
A2TMVαRxHC	0.1	FUT 11	0.05
A2PVXαRxLC	0.1	CMAS	0.05
A2TMVαKBPAHC	0.1	GNE	0.05
A2TMVαKBPALC	0.1	NANS	0.05
CST	0.05	STGALT	0.05
ST	0.05	GnTII	0.34
pC144	0.05	pG371	0.05
pPT2M-J-Chain	0.34	ERp44	0.12
p27A1AT	0.01	RCSeRNAihexo3	0.3
RCSeRNAihexo3+1	0.3		

Infiltrated leaves should be fully expanded, young leaves (2-3 first leaves infiltrated). Infiltration was performed with needleless 1 ml sterile plastic syringes, while applying slight pressure on the opposite leaf surface of the infected area (figure 11). Plants were let to grow for 3-5 days before harvested, depending on the infiltrated construct.

Figure 11: Plant agroinfiltration

2.2.5 Cloning of RNAihexo3

Minipreps were prepared out of overnight cultures of pMA-TNbHexo3 and SAT4. pMA-TNbHexo3 was digested with *KpnI*-HF and *BamHI*-HF and the 440bp fragment containing XTI2 intron and the 235bp antisense Hexo3 (asHexo3) was cleaned by gel purification kit procedure. The SAT4 vector was digested with the same enzyme pair, dephosphorylated according to procedure, and cleaned.

AsHexo3 fragment was ligated to SAT4 according to procedure and transformed into *E. coli*. Cells were then plated in agar containing ampicillin and incubated overnight at 37℃.

Colonies were screened with SAT4-F1/SAT4-R1 primers and positives (showing 650 bp) were grown in LB media supplemented with ampicillin overnight for miniprep preparation. The resulting plasmid SAT4asHexo3 was sequenced to confirm sequence.

p31Hexo3 minipreps were used as template to amplify the sense 235bp fragment from *N. benthamiana hexo3* using the primers ssHexo3-F1/ssHexo3-R1. PCR product was digested with *Xho*I and *Kpn*I-HF enzymes, and cleaned.

Minipreps of SAT4asHexo3 were then digested with *Xho*I and *Kpn*I-HF enzymes, dephosphorylated and cleaned with PCR purification cleaning kit.

The sense Hexo3 fragment was ligated to SAT4asHexo3 and transformed as previously described. Colonies were then screened with primer pair SAT4-F1/SAT4-R1 and positives were cultured overnight for miniprep preparation. Test digestions of the minipreps were done with *EcoRV* and *BamHI*-HF (expecting 900 bp positives) and sent for sequencing to ensure that no mutations are present.

The resulting plasmid SAT4Hexo3RNAi construct was digested with I-*SceI* enzyme, ran on an electrophoresis gel and 1.8 Kbp bands were cut and clean.

Clean bands were ligated to RCS vector digested with I-*SceI* and dephosphorylated. *E. coli* cells were transformed with this ligation, plated in agar supplemented with spectinomycin and screened with RCS2-F2/ SAT4-R1. Positive colonies were grown overnight, minipreps were prepared and test digested with *KpnI*-HF (expecting 1260 bp) to check orientation of insertion. The resulting vector Hexo3RNAi was finally transformed into *Agrobacterium tumefaciens*.

2.2.6 Cloning of RNAihexo1

A synthetic clone carrying the XTI2 intron and the 236bp antisence sequence of *N. benthamiana hexo1* flanked by *Xho*I-*Bam*HI sites (asHexo1) was transformed into *E. coli*. Colonies were grown overnight and minipreps were prepared.

Minipreps were digested with *XhoI* and *BamHI*-HF, the digestion was run in an electrophoresis gel and the 470 bp fragment was cleaned. The clean DNA was ligated to SAT1 vector digested the same way and dephosphorylated. After *E. coli* transformation and plating, colonies were screened with SAT1-F1/SAT1-R1 primer pair. Positive colonies were grown overnight, minipreps were prepared and sequenced (SAT1asHexo1).

A miniprep of p31Hexo1 was used for PCR amplification of the Hexo1 sense sequence with the ssHexo1-F1/ ssHexo1-R1 primer pair. PCR product digested with *XhoI* and *KpnI*-HF. After cleaning, the fragment was ligated to SAT1asHexo1 digested the same way, dephosphorylated and clean.

E. coli cells were then transformed with this construct, plated and positive transformants were screened with SAT1F-F1/SAT1-R1 (expecting 830bp). Positive colonies were cultured overnight, and minipreps were made. After test digestion with *BgL*II-*Bam*HI-HF, the resulting plasmid (SAT1Hexo1RNAi) was sequenced with SAT1-F1/SAT1-R1.

The expression cassette was excised by digestion with *Asc*I, ran on an electrophoresis gel and the band cleaned (1.8 Kbp). The RNAiHexo1 cassette was assembled in RCSeRNAiHexo3, digested with the same enzyme and dephosphorylated.

Colonies were then screened with epsps-F3/SAT1-R1. Positives were grown, minipreps were prepared, test digested with *XhoI* and transformed into *A. tumefaciens* .

3 Results

3.1 IgG upscaling and glycoengineering

Taking advantage from the fact that plant can glycosylate proteins in a vary homogenous way and that they are highly susceptible for glycoengineering, a scheme was setup to produce the mAb Rituximab with defined glycosylation profiles aiming to compare the impact of particular sugars on the mAb activity. With this it is expected that the therapeutic efficacy of mAbs may be optimized by the selection of a glycoform that best suits a particular function.

3.1.1 Small scale control of glycoengineering

Before large scale purification of recombinant Rituximab, small scale samples of infiltrated plant tissue (400 mg) were taken and purified for glycan analysis. This was aimed to verify if Rituximab was expressed and if the desired glycan profiles were being generated by the infiltrated glycoengineering constructs or stable transformed plant lines.

3.1.1.1 GnGn glycoform

For the GnGn (terminal GlcNAc) glycoform, ΔXF (without plant core xylose or fucose) plants were infiltrated with the magnICON® constructs for expression of Rituximab heavy and light chains. As this was the basic N-glycan expected, no other glycoengineering construct was infiltrated. Figure 12 shows the result from the SDS-PAGE and glycan analysis.

LC-ESI-MS glycan profiling shows a very homogenous glycosylation pattern on the Fc domain of Rituximab. 17% of the mAb is produced un-glycosylated, while hybrid structures (MGn) accounts for 9.5% and the targeted complex glycoform (GnGn) for 73.5%. Contrary to other mAb expressed in *N. benthamiana* ΔXF plants no leakage of core fucose is observed.

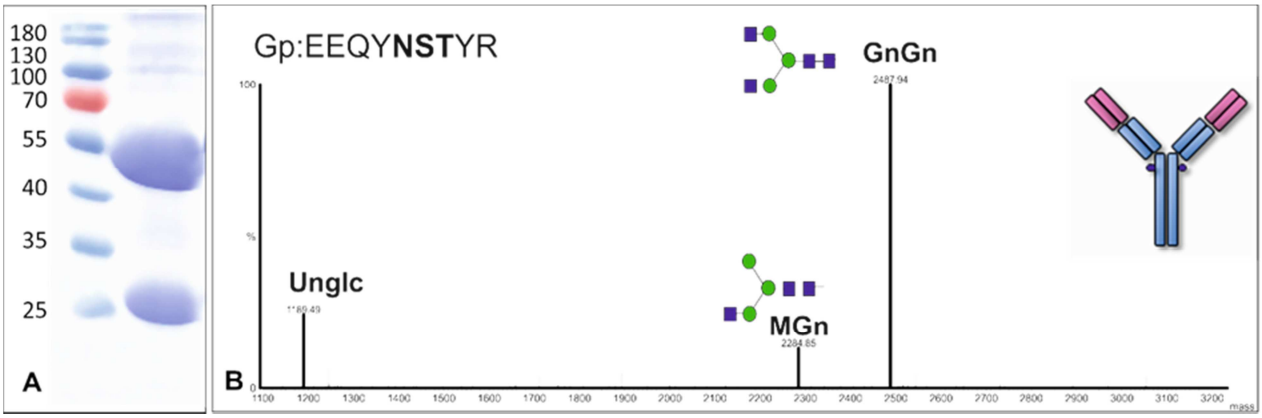

Figure 12: Small scale purification and glycan analysis of Rituximab expressed in *N. benthamiana* ∆XF plants. (A) SDS-PAGE followed by Coomassie Brilliant Blue staining of reduced sample shows two bands of ~55 and 25 KDa corresponding to the heavy and light chain respectively. (B) N-glycosylation profiling by LC-ESI-MS of tryptic Fc glycopeptide (EEQYNSTYR) confirms a great majority of the antibody decorated with the targeted GnGn glycoform. Peaks were labelled in accordance with the ProGlycAn system (www.proglycan.com). Schematic representations of N-glycans structures detected are also shown. Plant material was then used for large scale purification and quantification.

3.1.1.2 GnGnF glycoform

Rituximab carrying GnGnF glycans was produced to study the impact of core fucosylation. Also a recent study shown that mAb- Fc glycan processing largely depend on the presence of core fucose. In particular processing of the Fc glycosylation towards di-sialylated structures is largely improved in the presence of core α 1,3-fucose (Castilho et al., 2015).

Here we aimed to produce asialo-Rituximab with core fucosylation aiming to later compare to the sialylated and fucosylated version of Rituximab.

For the production of Rituximab GnGnF glycoform (terminal GlcNAc with plant core α1,3-fucose), the heavy and light chain constructs were co-infiltrated with the FUT11 construct in ∆XF plants.

Results are shown in figure 13. As before, we were able to produce the mAb with a very homogenous glycosylation and mainly carrying the desired glycoform. 23 % are un-glycosylated, 48% are complex fucosylated (GnGnF) and 7% of glycans are hybrid fucosylated (MGnF).

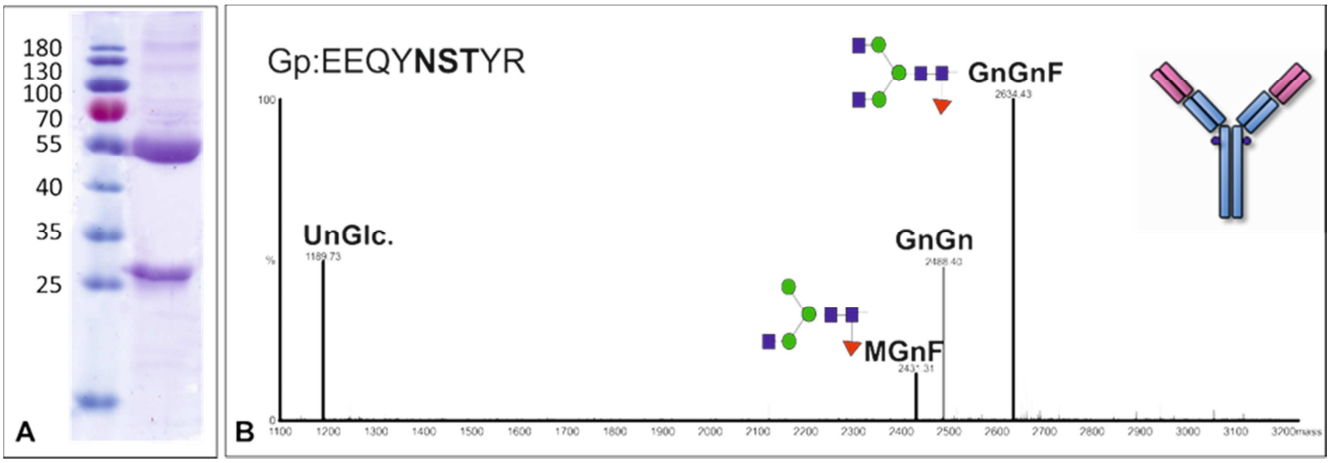

Figure 13: Small scale purification and glycan analysis of Rituximab co-expressed in *N. benthamiana* ΔXF plants with the α1,3-fucosyltransferase. (A) SDS-PAGE followed by Coomassie Brilliant Blue staining of reduced sample shows two bands of ~55 and 25 KDa corresponding to the heavy and light chain respectively. (B) N-glycosylation profiling by LC-ESI-MS of tryptic Fc glycopeptide (EEQYNSTYR) confirms a great majority of the antibody decorated with the targeted GnGnF glycoform. Peaks were labelled in accordance with the ProGlycAn system (www.proglycan.com). Schematic representations of N-glycans structures detected are also shown. Plant material was then used for large scale purification and quantification.

3.1.1.3 AA glycoform

The major glycans of recombinant IgGs contain 0, 1 or 2 terminal galactose residues and their relative proportions may vary depending on the cell culture conditions in which they were expressed. In fact, the heterogeneity of the glycosylation of Rituximab is mainly due to the variable presence of terminal galactose residues (Schiestl et al., 2011).

To produce di-galactosylated (AA) Rituximab, the heavy and light chains of the antibody were co-expressed with the STGalT construct (Strasser et al., 2009) in the ΔXF line. Figure 14 shows the results of the SDS-PAGE gel and the glycan analysis.

Plant-derived Rituximab is glycosylated in a homogenous way with 17.4% being unglycosylated and 11.2% high mannose glycans. From the complex glycans 29% are mono-galactosylated structures (MA and GnA) and 42% are di-galactosylated.

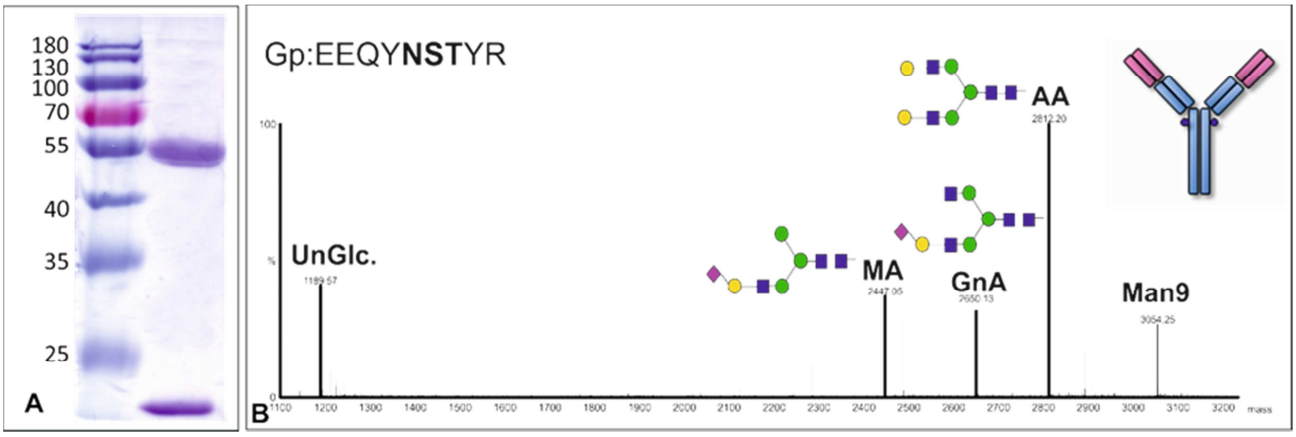

Figure 14: Small scale purification and glycan analysis of Rituximab co-expressed in *N. benthamiana* ΔXF plants with the STGalT. (A) SDS-PAGE followed by Coomassie Brilliant Blue staining of reduced sample shows two bands of ~55 and 25 KDa corresponding to the heavy and light chain respectively.

(B) N-glycosylation profiling by LC-ESI-MS of tryptic Fc glycopeptide (EEQYNSTYR) confirms a great majority of the antibody decorated with the targeted AA glycoform. Peaks were labelled in accordance with the ProGlycAn system (www.proglycan.com). Schematic representations of N-glycans structures detected are also shown. Plant material was then used for large scale purification and quantification.

3.1.1.4 NaNaF glycoform

In a recent study it was shown that mAb-Fc glycan processing largely depend on the presence of core fucose. In particular, processing of the Fc glycosylation towards di-sialylated structures is largely improved in the presence of core α 1,3-fucose (figure 15) (Castilho et al., 2015).

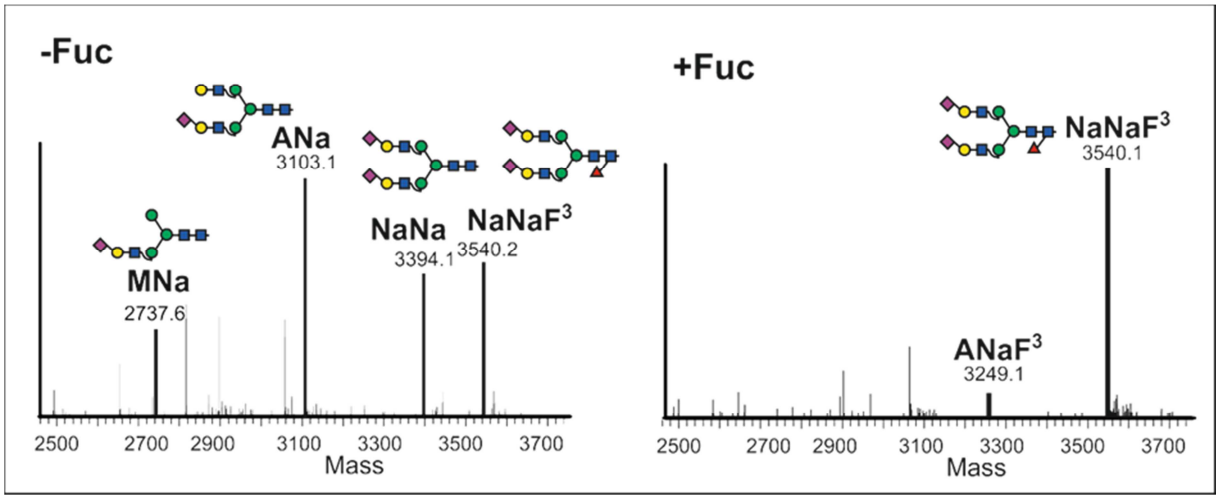

Figure 15: Monoclonal antibody co-expressed in *N. benthamiana* ΔXT/FT plants without (-Fuc) or with α1,3-fucosyltransferase. N-glycosylation profiling by LC-ESI-MS of tryptic Fc glycopeptide (EEQYNSTYR). Peaks were labelled in accordance with the ProGlycAn system (www.proglycan.com). Schematic representations of N-glycans structures detected are also shown. (Adapted from (Castilho et al., 2015))

It seems that the structures located in the Fc fragment are largely shielded by the opposing CH2 fragment. Molecular modelling suggests that core fucosylation strengthens the interaction between the two homologous Fc domains through glycan chains thus potentially influencing the entire glycan conformation. As a consequence the Fc- glycans may become more accessible for glycan processing enzymes (Castilho et al., 2015). For sialylation, several distinct methods of infiltration were tested (table 8). In all methods *Arabidopsis thaliana* α1,3-fucosyltransferase gene (FUT11) was co-infiltrated with Rituximab. In method 1 ΔXF mutants were used as hosts. Sialylation was achieved by the co-expression of two multiple binary vectors carrying the expression cassettes for the six necessary genes for in planta protein sialylation (Ce144 and Gb371, (Castilho et al., 2013)). In method 2 a new plant expression platform, where the pCe144 (figure 16) vector was used to stable transform ΔXF plants, was employed as host. This platform stably expresses the GNE, NANS and CMAS genes and is able to synthetize active sialic acid *in planta* (data not published). The Ce144 host was infiltrated with Gb371 multi gene vector (figure 16) to

allow Rituximab sialylation. In method 3 the original procedure (Castilho et al., 2010) where the Rituximab was co-infiltrated with all six genes individually was followed (figure 17).

Table 8: Tested infiltration methods for achieving NaNaF glycoform

Method	Glycoengineering Constructs	Plant Host
1	pG371 + pC144 Fut11	ΔXF
2	pG371 Fut11	Ce144
3	GNE GalT CMP NANS ST CMAS Fut11	ΔXF

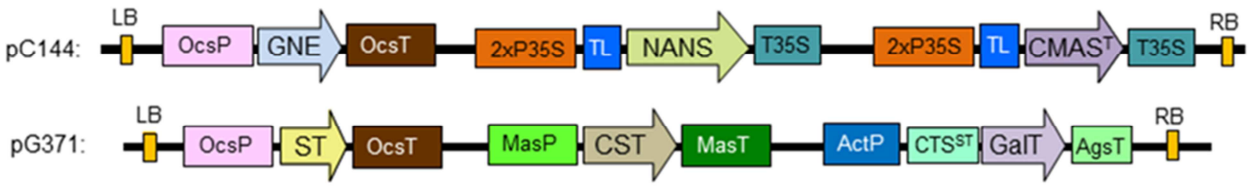

Figure 16: Schematic representation of the multi-gene vectors used in this investigation.35SP: cauliflower mosaic virus (CaMV) 35S promoter; TL: translational enhancer 5'-UTR from tobacco etch; 35ST: CaMV 35S terminator; OcsP: octopine synthase promoter; OcsT: octopine synthase terminator; actP: actin promoter; agsT: agropin synthase terminator; masP: manopine synthase promoter masT: manopine synthase terminator; GNE: mouse UDP-N-acetylglucosamine-2-epimerase/N-acetylmannosamine kinase; NANS: Homo sapiens N-acetylneuraminic acid phosphate synthase; CMAS: Homo sapiens CMP-N-acetylneuraminic acid synthase; STGalT: β1,4-galactosyltransfease fused to the cytoplasmic tail, transmembrane domain and stem region of the rat α2,6-sialyltransferase; CST: Mouse CMP-sialic acid transporter; ST: rat α2,6-sialyltransferase; LB: left border; RB: right border (adapted from (Castilho et al., 2013))

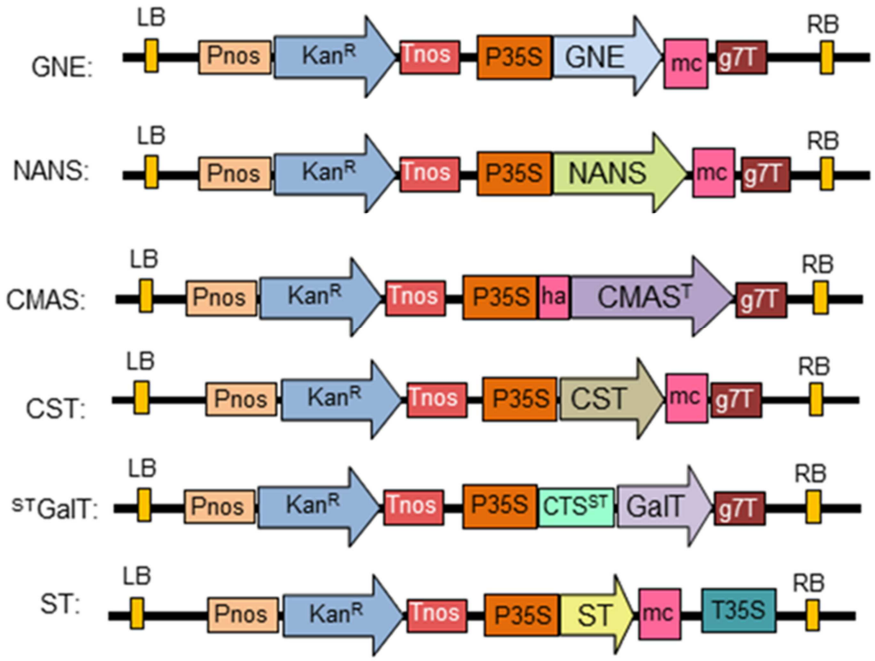

Figure 17: Schematic representation of the sialylation individual vectors used in this investigation. Pnos: nopaline synthase gene promoter; Tnos: nopaline synthase gene terminator; KanR: neomycin phosphotransferase II gene; P35S: Cauliflower Mosaic Virus promoter; g7T: agrobacterium gene 7 terminator; CTS: cytoplasmic tail-transmembrane-stem region; mc: c-myc epitope tag; ha: Hemagglutinin epitope tag; GNE: mouse UDP-N-acetylglucosamine-2-epimerase/N-acetylmannosamine kinase; NANS: Homo sapiens N-acetylneuraminic acid phosphate synthase; CMAS: Homo sapiens CMP-N-acetylneuraminic acid synthase; STGalT: β1,4-galactosyltransfease fused to the cytoplasmic tail, transmembrane domain and stem region of the rat α2,6-sialyltransferase; CST: Mouse CMP-sialic acid transporter; ST: rat α2,6-sialyltransferase; LB: left border; RB: right border. (Adapted from (Castilho et al., 2010))

Figure 18 shows the glycosylation profile of Rituximab expressed by the 3 methods.

Although in all methods Rituximab is mainly decorated with fucosylated di-sialylated glycans (NaNaF) the profile is much more homogenous when method 3 is used. The fraction of non- or mono-sialylated glycans is significantly higher in methods 1 and 2. As it can be seen, method 3 showed a more homogenous glycan profile, with a majority of the attached N-glycans being of the NaNaF type.

With method 3, un-glycosylated antibody accounts for 20.7%. The non-sialylated forms constitute 22.2% of the sample, mono-sialylated (MNaF) 12.7% and di-sialylated 43.6% (NaNaF).

For this reason method 3 was used for the large scale infiltrations and purification.

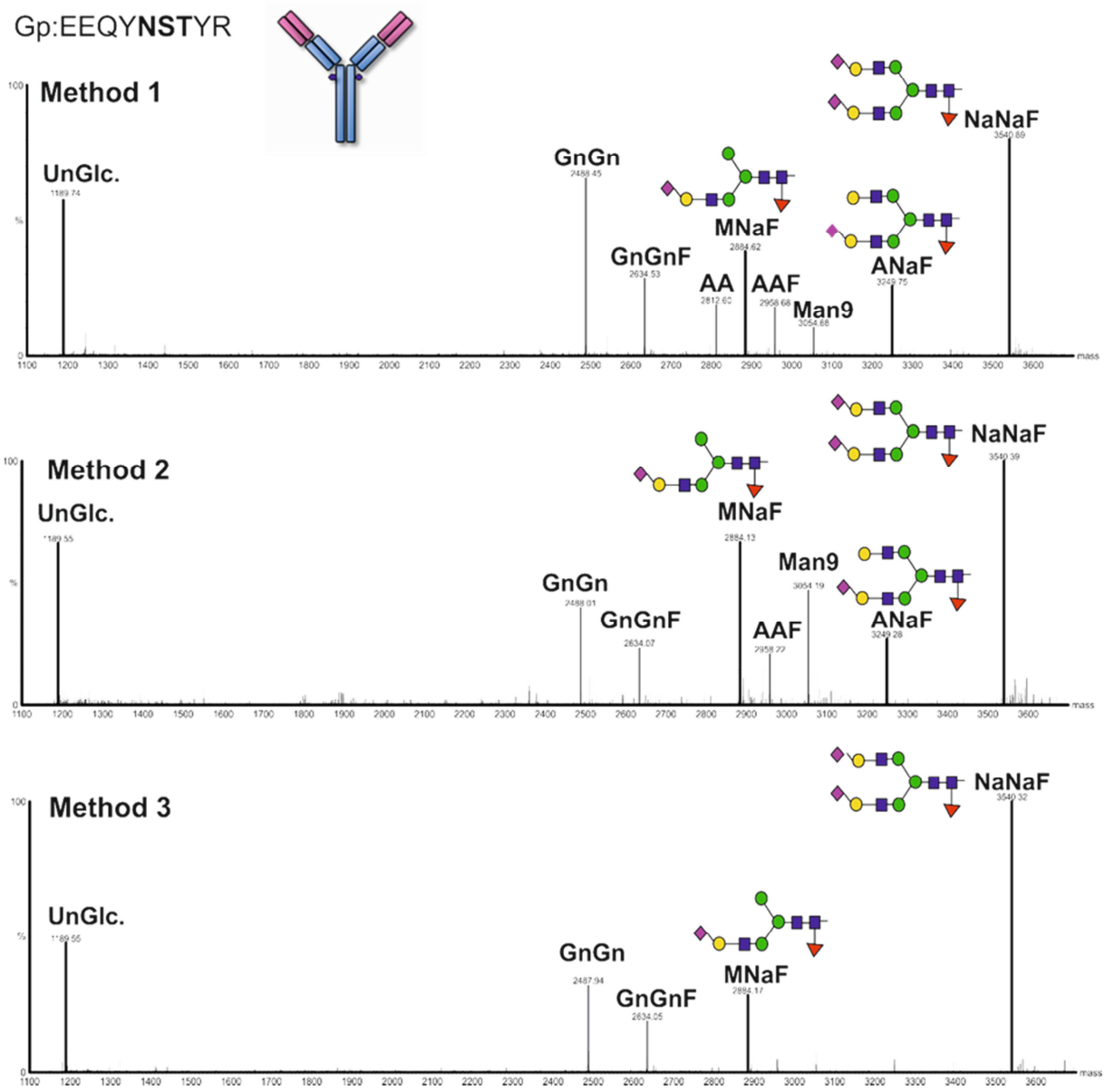

Figure 18: Small scale purification and glycan analysis of Rituximab co-expressed in *N. benthamiana* with the mammalian sialic acid pathway. Sialylation of Rituximab was attempted using three different methods summarised in Table 12. N-glycosylation profiling by LC-ESI-MS of tryptic Fc glycopeptide (EEQYNSTYR) confirms a great majority of the antibody decorated with the targeted NaNaF glycoform but glycosylation profile was more homogenous in method 3. Peaks were labelled in accordance with the ProGlycAn system (www.proglycan.com). Schematic representations of N-glycans structures detected are also shown. Plant material was then used for large scale purification and quantification.

3.1.2 Upscaling and purification

3.1.2.1 GnGn glycoform

Large scale infiltrations were performed the same way as the small scale infiltrations. 100 g of leaf material were used for purification as described in 2.2.3. After purification, SDS-PAGE gels of the dialysed elutions were run for quality control, together with crude extract, flow through and wash flow through samples. Afterwards, bands from the SDS-PAGE gel were sent for glycan analysis as described in 2.2.3. Since glycan profiles were similar to the

ones displayed in the small scale purifications, only the SDS-PAGE gels of the large scale purifications will be shown, together with the crude extract, flow through and wash flow through samples for quality control (figure 19).

The crude extract is expected to contain the soluble proteins, with a prominent band at around 55 kDa, corresponding to the size of the large sub-unit of RuBisCO. The flow through is expected to be like the crude extract, meaning that except for the target protein, all the other protein content has passed through the purification column but did not bind to the resin. As for the wash flow through, it should contain little to no protein content. This is precisely what is observed, with elution samples showing clean bands corresponding to heavy and light chain were obtained.

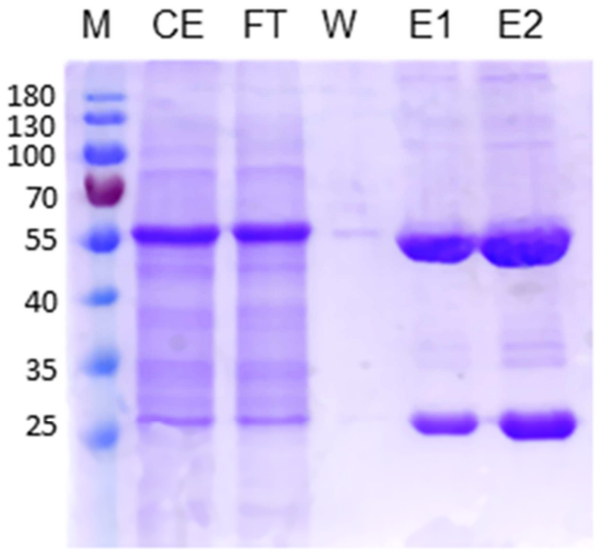

Figure 19: SDS-PAGE gel and Coomassie brilliant blue staining of Rituximab GnGn large scale purification. Ce, crude extract; FT, flow through; W, wash flow through; E1, elution 1 after dialysis; E2, elution 2 after dialysis.

After analysis, elution samples were then used for IgG quantification (see table 9).

3.1.2.2 GnGnF glycoform

Large scale infiltrations were performed the same way as the small scale infiltrations. 163 g of leaf material were used. SDS-PAGE results can be seen in figure 20.

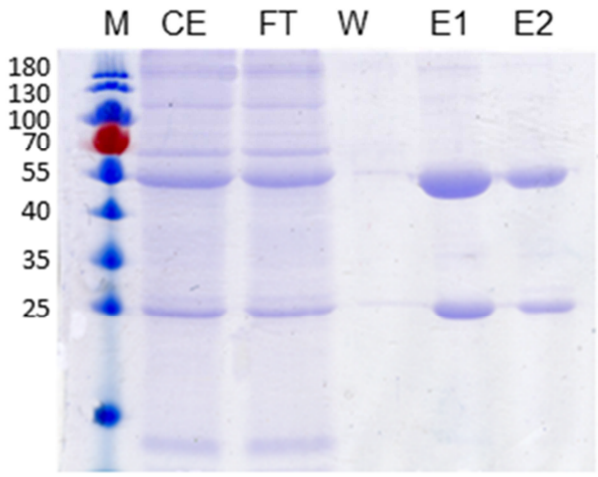

Figure 20: SDS-PAGE gel and Coomassie brilliant blue staining of Rituximab GnGnF large scale purification. Ce, crude extract; FT, flow through; W, wash flow through; E1, elution 1 after dialysis; E2, elution 2 after dialysis

The elution samples were quantified (see table 9).

3.1.2.3 AA glycoform

54 g of leaf material were used for purification. SDS-PAGE results are shown in figure 21.

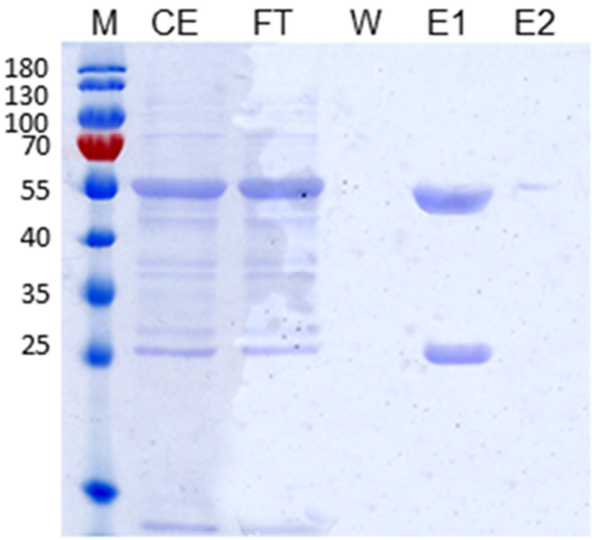

Figure 21: SDS-PAGE gel and Coomassie brilliant blue staining of Rituximab AA large scale purification. Ce, crude extract; FT, flow through; W, wash flow through; E1, elution 1 after dialysis; E2, elution 2 after dialysis.

The second elution of the purification did not result in a visible amount of protein. Therefore, only the first elution was quantified and sent for activity assays (see table 9).

3.1.2.4 NaNaF glycoform

As determined in 3.1.1.4, large scale infiltrations for the NaNaF glycoform were done according to method 3, which produced the most homogenous glycan profile. The results of SDS-PAGE can be seen in figure 22.

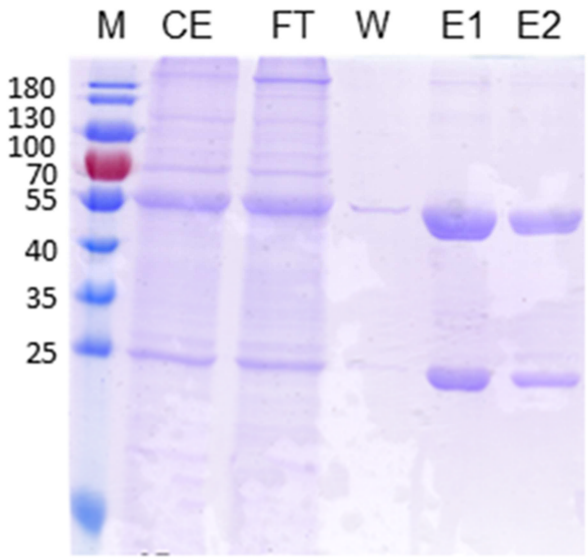

Figure 22: SDS-PAGE gel and Coomassie brilliant blue staining of rituximab NaNaF large scale purification. Ce, crude extract; FT, flow through; W, wash flow through; E1, elution 1 after dialysis; E2, elution 2 after dialysis.

Both elutions of the purification were then used for quantification (table 9).

3.1.3 Quantification of large scale protein yield

Quantification and yield of purified recombinant Rituximab is summarized in table 9. After quantification samples were sent for activity analysis.

Table 9: Quantification of purified protein and yield according to leaf tissue used

Dominant Glycan	Leaf Tissue Used (g)	Amount purified (mg)	Yield (µg/g)
GnGn	100	25.200	252
GnGnF	163	26.996	166
AA	54	5.848	108
NaNaF	178	20.680	116

The Rituximab purified samples produced in this investigation carrying different glycoforms were sent to our collaborators at Institute für Phamakologie, INO-F in Switzerland for further analysis. We aim to study the implications of specific sugar moieties of the glycan on Fc effector functions.

3.2 IgM upscaling and glycoengineering

The generation of IgMs with a controlled glycosylation pattern allows the study of the so far unknown contribution of sugar moieties to the function of IgMs.

As for IgG we aimed to produce KBPA with homogenous glycan profiles: GnGn (terminal GlcNAc) and NaNa (terminal sialylated). To achieve these glycoforms, infiltrations were done the same way as for the IgG. However, for IgM, heavy and light chains were co-infiltrated with the pPT2M-J-Chain and ERp44 constructs, to achieve a pentameric/hexameric oligomerization. Furthermore, agroinfiltration for the NaNa glycoform was done according to method 3 but the FUT11 construct was not added, since there are no evidence that core fucosylation enhances sialylation of IgMs (data not published). As described previously small scale purifications were done to assure that the target glycosylation profile was succeeded and this was followed by KBPA large scale infiltrations and purifications.

KBPA has 3 complex and 2 high-mannosidic *N*-glycosylation sites. Here we showed as representatives the glycan profiles for glycopeptide 2 (complex) and 4 (high mannose).

3.2.1 Upscaling and purification

3.2.1.1 GnGn glycoform

76 g of leaf tissue were infiltrated and then used for purification. Having one more domain in the heavy chain, the correspondent band on an SDS-PAGE gel is expected to be bigger, at 72 kDa.

Results of purification and glycosylation analysis can be seen in figure 23.

Using ΔXFT plants as expression hosts resulted in the production of KBPA carrying oligomannosidic N-glycans on glycopeptides 4 and 5, and human-type complex GnGn structures lacking plant-specific xylose and fucose residues at glycopeptides 1–3. Complex sites are decorated with the target GnGn (45.3%) glycoform although significant amounts of oligomannosidic glycans are also detected (54.7% for Man8 and Man 9). As expected on glycopeptides 4 and 5 no complex glycans are observed.

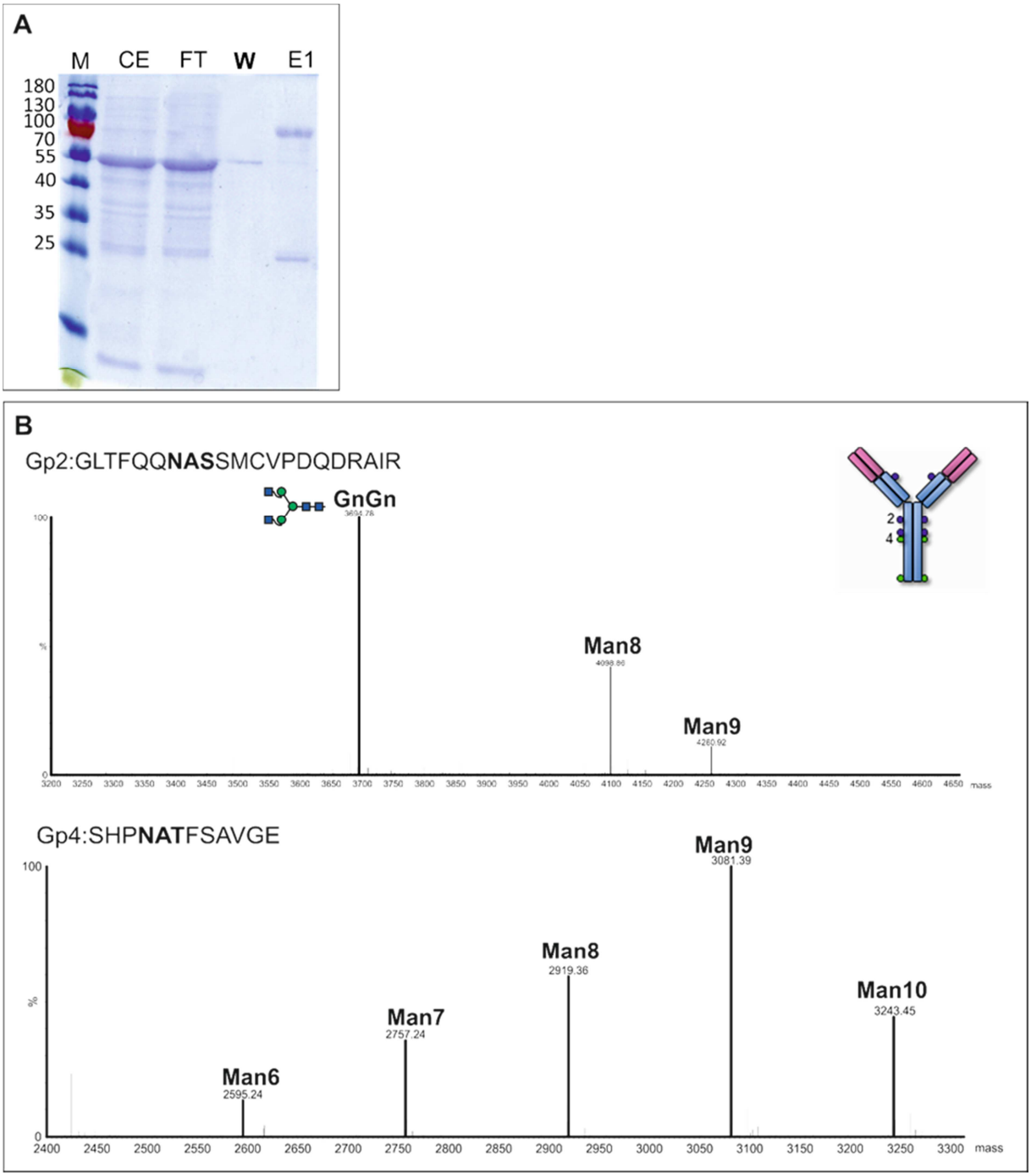

Figure 23: Large scale purification and glycan analysis of KBPA expressed in *N. benthamiana* ΔXF plants. (A) SDS-PAGE followed by Coomassie Brilliant Blue staining of reduced elution sample shows two bands of ~70 and 25 KDa corresponding to the heavy and light chain respectively. Ce, crude extract; FT, flow through; W, wash flow through; E1, elution 1 after dialysis. (B) N-glycosylation profiling by LC-ESI-MS of tryptic Fc glycopeptides 2 confirms a great majority of the antibody decorated with the targeted GnGn glycoform. As expected Gp4 shows high mannosidic glycans. Peaks were labelled in accordance with the ProGlycAn system (www.proglycan.com). Schematic representations of N-glycans structures detected are also shown.

The elution was used for glycan analysis and purification (see table 10).

3.2.1.2 NaNa glycoform

78g of infiltrated leaf tissue were used for purification. Both SDS-PAGE gel and glycan analysis can be seen in figure 24.

As before, purification is highly specific and both heavy and light chains are well visible on Coomassie stained gels. N-glycan analysis of the purified Fc revealed, as expected, the exclusive presence of oligomannosidic glycans on glycopeptides 4 and 5. KBPA is decorated with fully sialylated glycans (NaNa) on glycopeptide 2. However, this accounts for 26.6% of the total glycans, while oligomannosidic glycans represent 52.7% of the sample and 21% are non-engineered (GnGn) complex glycans.

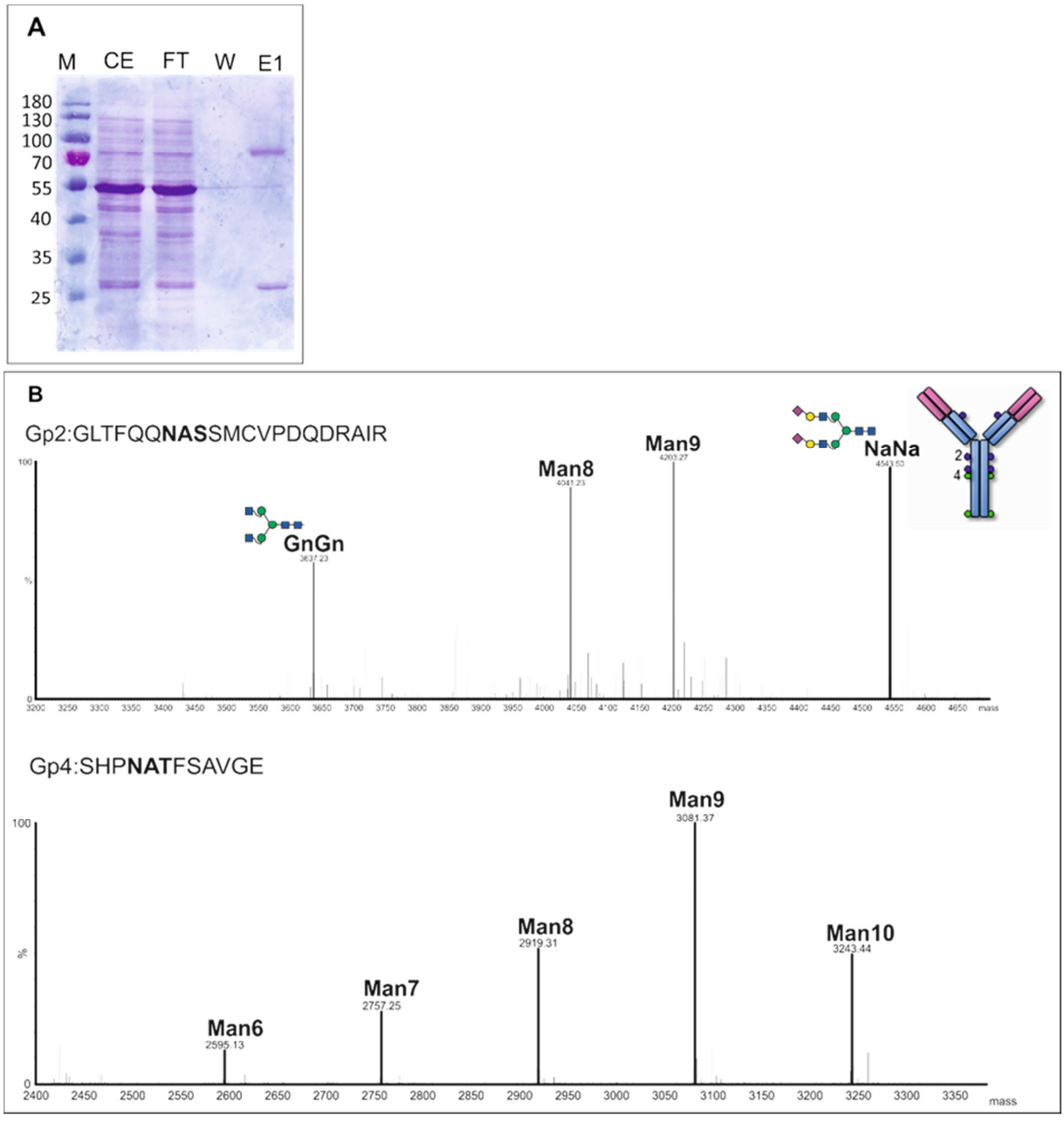

Figure 24: Large scale purification and glycan analysis of KBPA co-expressed in *N. benthamiana* ΔXF plants with the mammalian genes for in planta sialylation according to method 3. (A) SDS-PAGE followed by Coomassie Brilliant Blue staining of reduced elution sample shows two bands of ~70 and 25 KDa corresponding to the heavy and light chain respectively. Ce, crude extract; FT, flow through; W, wash flow through; E1, elution 1 after dialysis. (B) N-glycosylation profiling by LC-ESI-MS of tryptic Fc

glycopeptides 2 shows a fraction of antibody decorated with the targeted NaNa glycoform. High mannose and non-processed (GnGn) glycans are also detected. As expected Gp4 shows high mannosidic glycans. Peaks were labelled in accordance with the ProGlycAn system (www.proglycan.com). Schematic representations of N-glycans structures detected are also shown.

This sample was used for quantification (table 10).

3.2.2 Quantification of large scale protein yield

Quantification and yield of purified plant-derived KBPA is shown in table 10 according to the target glycan profile. After quantification samples will be used for further analysis.

Table 10: Quantification of purified protein and yield according to leaf tissue used

Glycoform	Leaf Tissue Used (g)	Amount Purified (mg)	Yield (µg/g)
GnGn	75	1.3	17
NaNa	78	4.7	60

The KBPA purified samples produced in this investigation carrying different glycoforms will be further analysed for their oligomerization status. To utilize the full potential as complement activator the desired IgM structure is the pentamer assembly. Due to time constrains this analysis was not possible during the course of this investigation. It is also aimed in a near future to characterize these samples through activity assays.

3.3 Down regulation of the expression of *N. benthamiana* Hexosaminidase 1 and 3

Two β-N-acetylhexosaminidases (HEXO1 and HEXO3) residing in different subcellular compartments jointly account for the formation of paucimannosidic N-glycans in *Arabidopsis thaliana*. HEXO1 is a soluble vacuolar protein and HEXO3 is largely insoluble and located in the plasma membrane and apoplast (Liebminger et al., 2011).

Although these truncated N-glycans are frequently found in plants, secreted recombinant glycoproteins usually carry complex N-glycans like GnGnXF or GnGn (depending on whether the expression host is WT or ΔXF). In our lab paucimannosidic N-glycans were observed on secreted α-1-anti-trypsin (A1AT, figure 5) (Castilho et al., 2014). This study showed that complex N-glycans of A1AT are converted to paucimannosidic structures, most probably in the extracellular space by the action of *N. benthamiana* HEXO3.

The identification of HEXO3 has being in the origin of undesired paucimannosidic structures decorating secreted recombinant proteins led us to design a construct with appropriate RNAi sequences to down regulate the activity of this enzyme in *N.*

benthamiana. In addition we also designed a construct to down regulate the activity of the vacuolar resident acetylhexosaminidase 1 (HEXO1).

3.3.1 Hexo3RNAi and Hexo3/1RNAi construct cloning

In collaboration with Dr. Richard Strasser (BOKU, Vienna) we have use the *N. benthamiana* potential sequence for *hexo3* to amplify a 235bp fragment and clone it sense/antisense to produce a RNA interference expression vector (figure 25A). In the same way, a 236 bp fragment of a potential sequence for *N. benthamiana hexo1* was cloned sense and antisence as described in sections 2.2.5 and 2.2.6 (figure 25A).

The pSAT-family vectors allow target sequences to be cloned under a large choice of promoters and terminators and the expression cassettes are easily interchangeable (Chung et al., 2005). The two different RNAi sequences were initially cloned into pSAT vector (1 and 4) and subsequently the expression cassettes were assembled in a binary vector carrying a 2mEpsps gene expression cassette for glyphosate resistance (figure 25B).

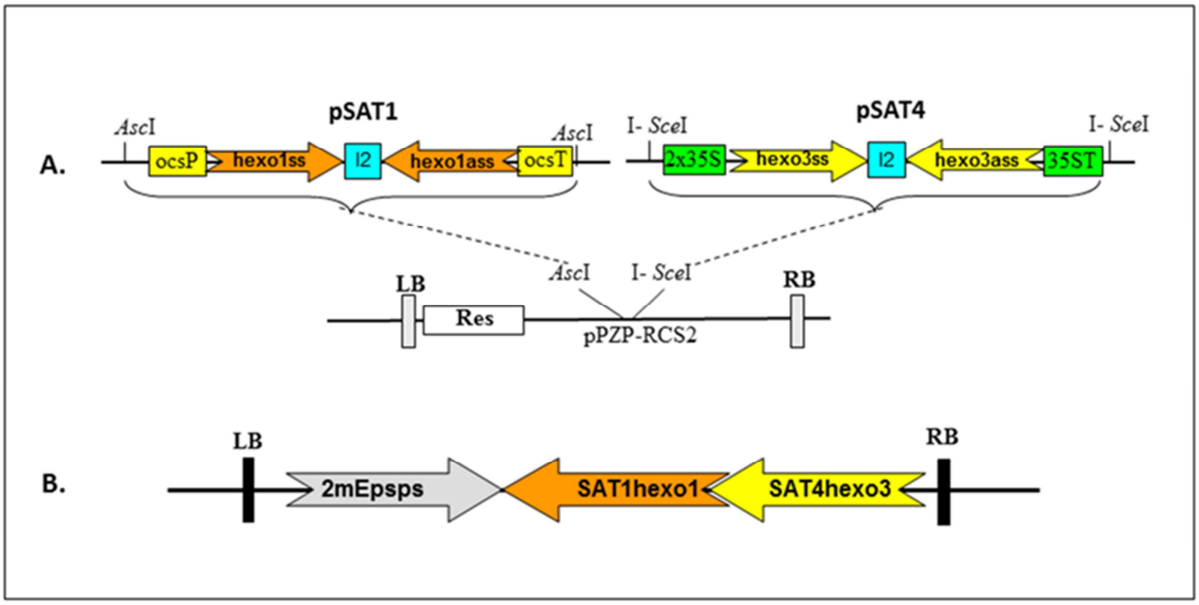

Figure 25: Cloning of Hexo 1 and Hexo 3-RNAi constructs. RNA interference constructs targeting the expression of endogenous β-N-acetylhexosaminidase 3 and 1 used for expression in *Nicotiana benthamiana*. (B) Outline of the cloning strategy of the Hexo1 and Hexo3 RNAi subcloned into pSAT auxiliary vectors and then sequentially assembled in pPZP-RCS2 using specific rare-cutting enzymes. (B) Schematic representation of the assembled Hexo 1 and Hexo3 RNAi sequences in the binary vector showing their relative orientation. P35S and T35S: cauliflower mosaic virus 35S promoter and terminator; OcsP and OcsT: octopine synthase promoter and terminator; I2: intron 2 from sequence of the Arabidopsis β1,2-xylosyltransferase gene (At5g55500); *hexo3* ss and *hexo3* ass: sense and antisense 235bp fragment of the potential *N. benthamiana Hexo3* gene; *hexo1* ss and *hexo1* ass: sense and antisense 236bp fragment of the potential *N. benthamiana hexo1* gene; 2mEpsps: 5-enolpyruvyl shikimate-3-phosphate synthase enzyme expression cassette for glyphosate resistance; LB: left border; RB: right border

The cassette for Hexo3 RNAi was first inserted into the binary vector giving rise to the single vector for down regulation of HEXO3. Next the Hexo3 RNAi vector was used to clone in the RNAi sequence for *hexo1* giving rise to the double vector Hexo3/1RNAi.

For the cloning procedure, every step was checked by screening PCR or test restriction digestions.

The primers used for screening, not only confirm that the cell colonies have been successfully transformed, but also indicate the orientation of the expression cassettes. All sequences were confirmed by DNA sequencing.

Figure 26 shows the final PCR screening results for the transformed *A. tumefaciens* colonies with Hexo3 and Hexo3/1 RNAi constructs.

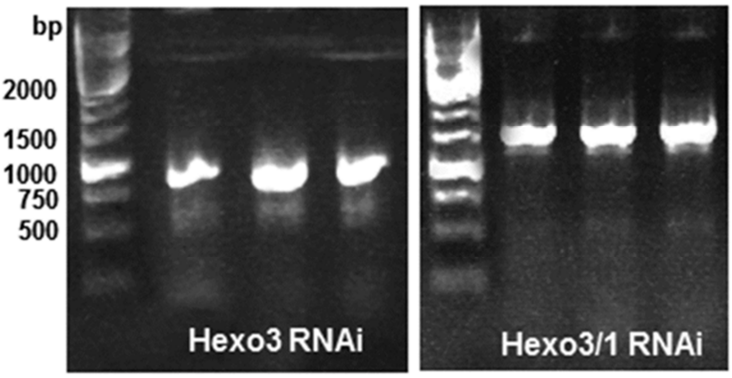

Figure 26: Electrophoresis gel of PCR product obtained from screening for *A. tumefaciens* colonies cloned transformed with the RCS vectors. In all cases the bands observed on the gels were of the expected size, and also the sequencing results were in concordance.

3.3.2 Down regulation of paucimannosidic glycans by Hexo3RNAi and Hexo3/1RNAi

To test the activity of the RNAi constructs, these were co-infiltrated with A1AT. As it is known that this protein displays truncated glycoforms when targeted for secretion, it is one of the contenders for testing the inhibition of hexosaminidase 3 activity. This was done in wild type and ΔXF plants. Hexosaminidase 1, as it is located in the vacuole, should not have any effect on A1AT and its activity inhibition must be tested on other studies, using a vacuole targeted protein as a reporter.

Figure 27 shows the glycan profiles of A1AT co-infiltrated in wild type and ΔXF plants with and without Hexo3 RNAi construct. Co-infiltration with Hexo3/1 RNAi constructs displayed similar results, showing that the presence of an extra cassette does not affect the expression of Hexo3 RNAi (data not shown).

In table 11, the relative abundance of each glycoform is displayed.

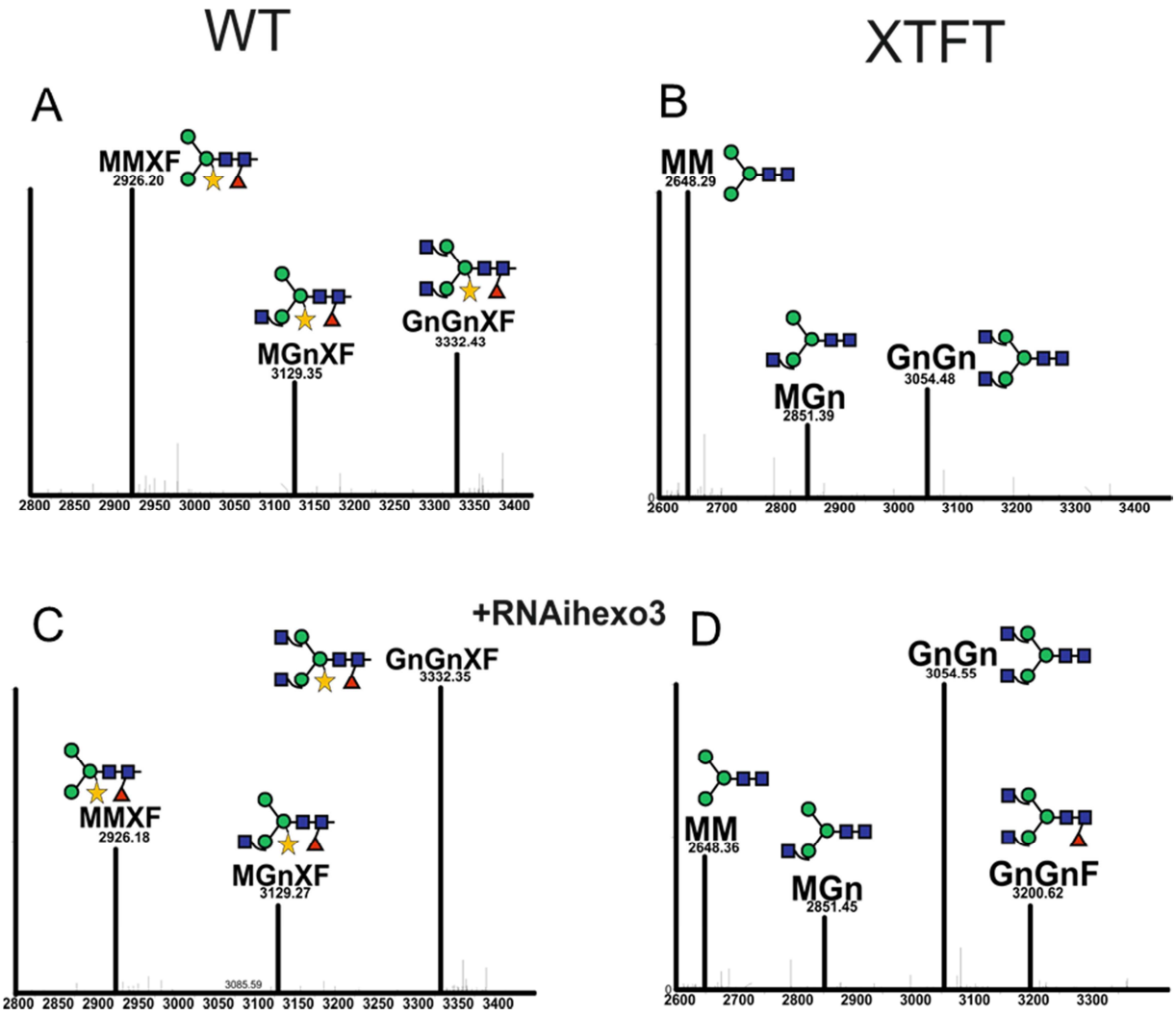

Figure 27: Secreted A1AT is decorated with Paucimannosidic N-glycans when expressed in both (A) wild type (WT) and in (B) glycosylation mutant plants (XTFT) (TOP PANEL). When co-expressed with the Hexo3 RNAi construct to downregulate the expression of *N. benthamiana* HEXO3, A1AT shows a significant increase in complex fully processed glycans (C. GnGnXF or D. GnGn). LC-ESI-MS of trypsin-digested A1AT collected from the intercellular fluid (IF). N-glycosylation profile of glycopeptide 2 (ADTHDEILEGLNFNLTEIPEAQIHEGFQELLR) is shown. Peaks were labelled using the ProGlycAn system (www.proglycan.com). Adjacent illustrations display the respective N-glycans using standard symbols.

Table 11: Variation of glycoform percentage in *N*-glycans of A1AT infiltrated with and without Hexo3 RNAi in both wild type and ΔXF plants.

Plant Line	Glycoform	% without RNAi hexo 3	% with RNAi hexo 3
Wild type	MMXF	45.7	26.3
	MGnXF	17.3	16.6
	GnGnXF	37.0	57.1
ΔXF	MM	35.8	18.6
	MGn	15.2	13.0
	GnGn	23.2	53.8
	GnGnF	8.6	14.6

Hexo3 RNAi also affected the plants' total glycosylation profiles. Figure 28 shows a deconvoluted glycan profile of total secreted protein from both wild type and ΔXF lines, with and without Hexo3 RNAi.

As seen, co-infiltration with Hexo3RNAi clearly shows a reversion of paucimannosidic structures in favour of fully processed glycans. This is a remarkable achievement since the down regulation of the target gene is done by transient expression only.

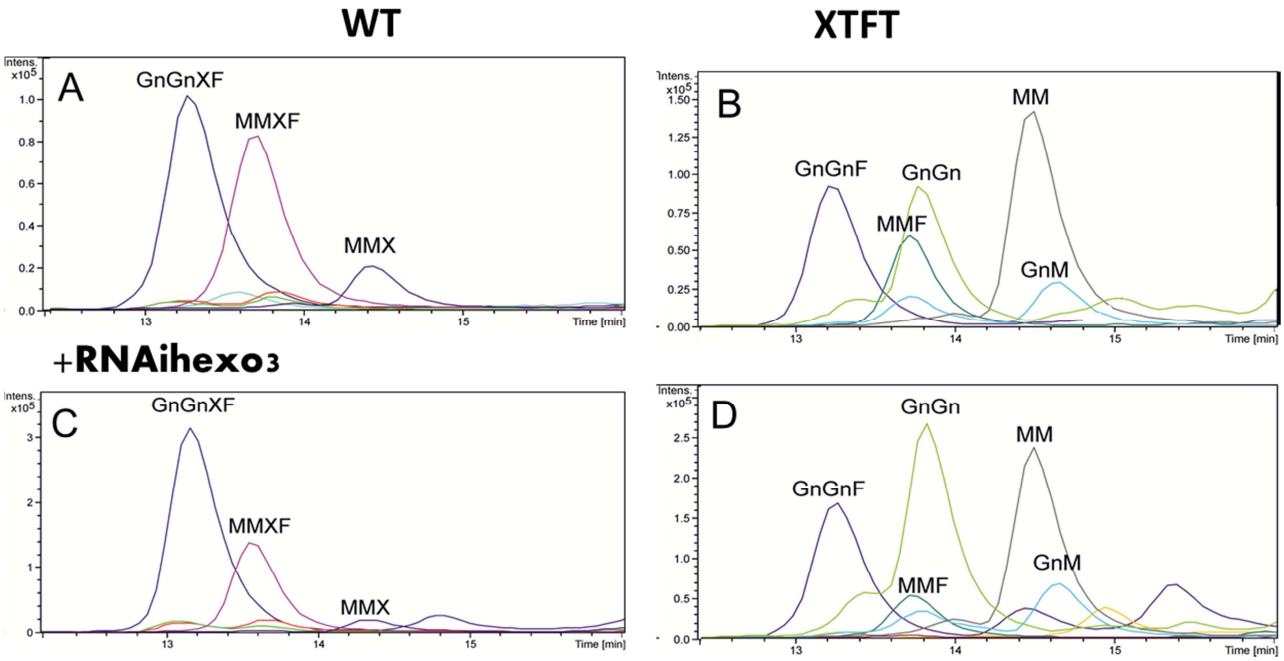

Figure 28: Glycan profiles from secreted protein. A, total secreted protein of wild type plants; B, total secreted protein of ΔXF plants; C, total secreted protein of wild type plants infiltrated with Hexo3 RNAi; D, total secreted protein of ΔXF plants infiltrated with Hexo3 RNAi.

4 Discussion

Plants are distant enough from humans that there are no common pathogens or similar proteins between the two. However, plants can still produce and assemble human like proteins in a correct way.

This fact can be employed for the establishment of a safe protein production system, with enough quantity, safety and homogeneity to satisfy the rising needs of human like proteins for medical purposes.

Fortunately, the magnifection technology developed by ICON genetics (magnICON), allows for an easy and productive way for recombinant protein synthesis.

The technology is based on the infiltration of plants with highly diluted agrobacterium suspensions carrying T-DNAs. These encode viral replicons and result in high copies of RNA molecules coding the desired protein. Since no gene is incorporated in the plant genome there are no risks of contamination or dissemination of the transgene (Klimyuk et al., 2014). The fact that the method enables the production of therapeutic and other high-

value recombinant proteins in non-GMO using non-food plants makes dealing with regulatory agencies more straightforward.

Adding to a good production system, glycoengineering can be used to control the glycosylation pattern of plant produced proteins (Bosch et al., 2013).

The true challenge consists in upscaling the plant produced protein process while maintaining homogenous glycosylation patterns.

As it is known that glycosylation influences the stability of proteins (Carrasco-Moro et al., 2009) and that by modulating the glycosylation of a protein its function can be amplified or diminished, it is of the utmost interest to combine glycoengineering with protein production in plants.

Plants glycosylate proteins differently than mammalian cells (Gomord et al., 2010). *N. benthamiana*, like other plants, produces essentially the same core glycan, but modified with xylose and fucose in a non-mammalian linkage (α1,3). With the development of *N. benthamiana* transgenic lines (ΔXF) depleted of plant glycoepitopes (Strasser et al., 2008; Strasser et al., 2009), magnICON technology can be coupled with glycoengineering to produce mAbs with glycoforms that are essentially mammalian-like. Indeed, the resulting glycoforms on mAbs produced in these plants are more homogeneous than many FDA-approved mAbs produced in mammalian cell culture (Whaley et al., 2011).

In a large scale, it is expected that this technology will allow for a fast and productive system, while keeping the product as clean and effective as possible. A good and promising example is the ebola antibody-based Immunotherapy. MAbs against the ebola virus, showed to protect against lethal ebola challenge in mice (Winkler et al., 2000) Manufacturing runs on large scale using magnICON vectors and ΔXF host *N. benthamiana* plants were done and proved effective (Zeitlin et al., 2011). Moreover, the glycosylation patterns (GnGn) resulted in improved efficacy compared to the identical mAb expressed in mammalian NS0 cells. Binding studies using Fc receptors revealed enhanced binding of non-fucosylated mAb to mouse and human Fc-RIIIa (mediating ADCC activity).

Antibody-based therapies have been widely used to treat many diseases including cancers, infectious and inflammatory disorders. The monoclonal antibodies produced by mammalian cells are humanized to avoid immunological responses but are heterogeneously glycosylated. The importance of glycosylation on the activity of the mAb by mediating the Fc interaction with receptors on the immune cells is well documented. Thus, it is a major goal to produce antibodies with well defined glycosylation, so it may be pssible to identify the one(s) that confer an improved safety and efficacy.

While it is clear that certain Fc glycans dramatically influence the binding to selected Fcγ receptors, studies on the effects of all known Fc glycan structures are beginning to emerge (Lin et al., 2015).

The finding that sialylation of Fc portion of an antibody can determine anti-inflammatory properties (Kaneko et al., 2006) provides new opportunities for enhancing the efficacy of current therapeutic immunoglobulins and for the development of new therapeutics. In addition, glycan analysis revealed a preferential 2,6-linkage in the IVIG preparations conferring anti-inflammatory activity (Anthony et al., 2008).

Current generation of licensed therapeutic mAbs carry oligosaccharides essentially devoid of sialic acid (Jefferis, 2006; Kobata, 2008). The extensive repertoire of glycosyltransferases and the fact that they can compete for the same substrate makes the Fc glycan profile tremendously heterogeneous. In humans, over 30 glycoforms on the single heavy chain have been identified (Jefferis, 2012). This microheterogeneity clearly complicates the investigation of the specific functionalities conferred by a single N-glycan residue. Using a combination of endoglycosidase to treat the antibody glycoforms and replace them by pure synthetic tailored glycans, it's possible to obtain a homogeneous antibody for activity assay (Lin et al., 2015). The comparison of the activity of Rituximab with several homogeneous glycoforms identified α-2,6-linked NaNa as the optimal structure to enhance the activities of antibodies against cancer, influenza, and inflammatory diseases.

Compared to IgGs, studies on the impact of glycosylation on IgM activity are overdue.

The possibility to efficiently produce different well-characterized IgMs glycoforms provides practical tools to elucidate the impact of glycosylation on the biological properties of IgMs. As for IgG, such studies may accelerate the generation of therapeutic proteins with optimized functions.

Due to their rather narrow range of glycosylation reactions, plants carry out complex N-glycosylation at a striking homogeneity, which makes them especially amenable to glyco-engineering (Steinkellner and Castilho, 2015).

The present investigation was built on the above mentioned idea. To identify the optimal glycan structures for individual antibodies with desired activity, we have developed an effective method to modify the Fc-glycan structures to a homogeneous glycoform.

The production of homogenously glycosylated antibodies was achieved taking advantage of the intrinsic properties of plant glycosylation and setting up a large scale laboratory experiment. While laboratory conditions are not suitable for big pharma, they are the ideal for emergency situations, when fast production of a usually uncommon biopharmaceutical is needed. As proved in this study, relatively large amounts of Rituximab (250µg/g) and KBPA (60µg/g) could be produce within 5 days even without optimization of the production system.

The glycosylation still proves to be a challenge. In each test infiltration, the engineered glycan structure was achieved. However, the efficiency of glycoengineering seems to

decrease when the complexity of the target glycan structure increases. Engineering complex structures like NaNaF results in a more heterogeneous profile for both IgG and IgM.

Another issue is the amount of un-glycosylated antibody. As seen for IgG, the amount of un-glycosylated antibody in each profile ranges from 5-25%. This phenomenon seems to be protein dependent since other plant-derived monoclonal antibodies display very little amounts of un-glycosylation (Castilho et al., 2010; Castilho et al., 2011a). Un-glycosylated antibodies display reduced effector functions, as well as reduced antiinflammatory properties, due to lower interaction with Fc receptors of effector cells (Lin et al., 2015). This is one of the issues to be addressed in future studies, and an effort should be made towards reducing un-glycosylation (see below).

Sialylated antibodies were successfully produced. More importantly, recent studies suggest that α2,6-linked terminal sialic acid glycans may improve antibody effector function (ADCC) and not only antiinflammatory properties (Lin et al., 2015) as it was previously thought. While the production of mAb decorated with mono-sialylated afucosylated glycans is possible, the profile are rather heterogeneous and di-sialylated afucosylated glycans account only for 15% of the glycans (Castilho et al., 2010; Castilho et al., 2015). The presence of core α1,3-linked fucose enhances the synthesis of di-sialylated glycans up to 90% (Castilho et al., 2015) but might have a negative effect on Fc receptor interactions and ADCC (Shields et al., 2002; Shinkawa et al., 2003; Okazaki et al., 2004). In this investigation plant-derived Rituximab was also efficiently decorated with di-sialylated core fucosylated glycans, at great uniformity. The main aim of producing Rituximab with sialylated glycans was to test the impact of sialylation on anti-inflammatory activity by comparing the GnGnF and NaNaF glycoforms. Nevertheless, since the recent report suggesting that α2,6-sialylation may improve ADCC, the next efforts should be put towards achieving maximum di-sialylation without having to add a core fucose residue.

While uniform glycosylation with the targeted glycan structures being the main form was easily achieved in Rituximab, the same was not true for KBPA-IgM. In this case both targeted glycoforms (GnGn and NaNa) were accompanied by significant portions of ER-typical oligomannosidic structures. Nonetheless, if one disregards the fraction of IgM ER-retained (Man8 and Man9 structures), secreted KBPA profiles are also highly homogenous with virtually one glycoform in di-sialylated (NaNa, 56 %) and non-converted (GnGn, 44 %) glycans.

Partial ER-retention of recombinant proteins targeted for secretion has been previously reported (Castilho et al., 2014; Schneider et al., 2014a). Recently it was shown that oligomerization status influenced subcellular localization and glycosylation of recombinant butyrylcholinesterase expressed in *N. benthamiana* (Schneider et al., 2014b). This and the

results presented here for IgM glycoengineering point for the need of in-depth studies to address the unexpected subcellular deposition of multimeric recombinant proteins in plants.

Another issue with plant-derived KBPA was the purification yield. Compared to Rituximab, KBPA expresses less. It must be kept in mind that fully assembled IgM antibodies are more complex and larger than IgG, which could pose additional expression, glycoengineering and purification difficulties. Nevertheless, IgMs are well expressed in plants and correctly assembled as multimeric proteins (Loos et al., 2014)

The affinity capture model that dominates IgG purification has proven not as efficient for IgMs because, in most cases, they are affected adversely by harsh elution conditions and they are more susceptible than IgGs to denaturation. (Garcia-Gonzalez et al., 1988). The large size of IgMs is also a challenge because it limits the operating conditions.

Purification of KBPA via Protein A affinity is possible but binding is very poorly compared to IgG and high protein levels are observed in the flow through. In addition, the binding of protein A-purified KBPA towards C1q receptor is jeopardised (unpublished data). Alternative purification protocols make use of affinity matrix containing ligands directed towards a unique domain on the Fc part of IgM as is CaptureSelect used in this investigation. It is however worth to point out that the binding capacity of the resin (2.5 mg IgM per mL matrix) is clearly less then protein A used for IgG (35 mg IgG per mL matrix). These and the distinct protein size may account for the significant differences in the purification yield of IgG and IgM. Improving and optimizing purification of plant-derived KBPA will no doubt be the focus of future research (see below).

From an industrial point of view, it is important to have an optimized antibody, maximizing its function. So, batch to batch reproducibility is extremely important soplant produced antibody can be glycosylated in the same way. Plants are the ideal platform for achieving this homogeneity. Being susceptible to glycoengineering and still a developing platform, there is much room for improvement. Using mutated plant lines that are stable transformed not to express certain glycosyltransferases like the *N. benthamiana* ΔXF line (Strasser et al., 2008) and transient expression for glyco-modulation, one can aim to achieve glycosylation patterns not possible to achieve in other platforms like CHO cells.

The formation of highly complex oligosaccharide structures like sialylation requires the coordinated expression of six human proteins acting in different subcellular compartments at different stages of the glycosylation pathway (Castilho et al., 2010). Castilho and co-workers were able to expresse Erythropoietin in ΔXF carrying branched sialylated N-glycans and mucin-type sialylated O-glycans with a total of 17 transiently expressed proteins (Castilho et al., 2012; Castilho et al., 2013). Although this seems extraordinary and exciting it is also prone to failure, as one cell must receive all the genes. It is also time consuming, involving handling of too many different *Agrobacterium* cultures. An obvious

approach to simplify the procedure (transient or stable) is to reduce the number of binary vectors that need to be co-delivered into plants. In planta synthesis of sialylated N-glycans by the transient expression of multigene vectors and thus reducing the number of agrobacteria in the infiltration process has been reported (Castilho et al., 2013; Schneider et al., 2014b). In a near future we aim at the glycan engineering approach by generating plants stably expressing the human sialylation pathway. Multigene transformation will no doubt become routine in plant biotechnology as researchers seek to introduce new and complex traits into plants.

Plant specific glycosydases are another obstacle to surpass if this platform is to be the leader of recombinant protein production. In this work, the down regulation of β-N-acetylhexosaminidase 3 expression was described. While not completely abolishing the protein expression, the expression of the RNAi constructs was enough to reduce paucimmanosidic glycans in A1AT by 42% in wild type plants and even more, 48%, in ΔXF plants. This represents a significant reduction in paucimmanosidic structures. Next steps should be employed to stable transform plants, knocking out the gene completely. While β-N-acetylhexosaminidase 1 was also studied, it is located in the vacuole, and this is not a target destination for produced proteins. Since most produced proteins are targeted for the glycosylation pathway and later secretion for the apoplast, it is for now more interesting to pursuit the inhibition of β-N-acetylhexosaminidase 3.

The present study addressed a series of current issues with the production of proteins in plant platforms. This still small and developing technology can still grow in many ways, and efforts must be made to improve it.

Controlling glycosylation in vivo through modulation of glycan biosynthesis can be a hurdle since the process has no known template and is dictated by many factors such as the availability, activity and correct sub-cellular localization of particular substrates and enzymes.

A common difficulty that impedes research on the impact of protein glycosylation to functional activities is availability of expression platforms that allow the synthesis of targeted glycoforms.

We have now available in our lab 4 plant-based expression platforms for the production of recombinant proteins with almost a single glycoform (WT: GnGnXF; ΔXTFT: GnGn; GalT: AA and Sia: NaNa, on its way). It is however important to acknowledge glycosylation is to a certain point protein specific and we have always to consider the “fine-tuning” of the glycoengineering procedure.

5 Future Prospects

The present study addressed a series of current issues with the production of proteins in plant platforms. This still small and developing technology can still grow in many ways, and efforts must be made to improve it.

5.1 OST expression

In eukaryotes, the key step of protein N-glycosylation in the endoplasmic reticulum is catalyzed by a multimeric protein complex oligosaccharyltransferase (OST). It transfers the lipid-linked core-oligosaccharide to selected Asn-X-Ser/Thr sequences of nascent polypeptide chains (see review in (Mohorko et al., 2011)). Due to the high substrate specificity of OST, alterations in the biosynthesis of the oligosaccharide or perturbation that destabilizes OST complexes can result in the hypoglycosylation of many different proteins (Mohorko et al., 2011).

Mammalian cells can express two isoforms of the OST catalytic subunit STT3 (STT3-A and STT3-B). A recent report showed that modulation of the STT3 isoform expression resulted in increased IgG N-glycosylation (Prados et al., 2011).

In this investigation we observed relatively high levels of unglycosylated IgG-Rituximab. The glycan analysis was done in tryptic peptides of reduced samples so levels of un-glycosylation may in fact reflect a mixture of non-glycosylated IgG with hemi-glycosylated IgG. Nevertheless, contrasting to other IgG expressed in *N. bethamiana* the same way, Rituximab is hypoglycosylated. One possible way to overcome this would be to try to co-express Rituximab with mammalian or plant OST. The approach was already attempted by ICON genetics with promising results (Dr. V. Klimyuk personal communication).

5.2 Improving/optimizing purification efficiency of IgMs

Purification of plant derived IgM proved to be more arduous. Enriched IgG product is easily obtained by Protein A affinity chromatography. Hydroxyapatite affinity seems to be provides a useful alternative for IgM (Gagnon, 2009). Either hydroxyapatite or cation exchange may support effective capture, depending on the properties of a particular IgM. Also we aim in a future to test other commercially available systems such as HiTrap IgM Purification HP (GE healthcare) packed with a thiophilic adsorption medium with 2-mercaptopyridine having a binding capacity of 5 mg human IgM per mL. Additionally, with the recent information obtained on IgM glycosylation (bisected sialylated), the next aim should be to glycoengineer the human serum glycan structures in plant produced recombinant IgMs.

5.3 Plant expression platform for protein sialylation

In collaboration with our partners at Icon Genetics (Halle, Germany) we have individually transformed the pC144 and pGb371 into the genome of *Nicotiana benthamiana* glycosylation mutant. Transformed Ce144 and Gb371 lines were crossed and progeny thereof tested by *Sambucus nigra* lectin (SNA) blotting, detecting di-sialylated proteins (NaNa). In addition and taking advantage of the different resistance cassettes present in the vectors we have co-transformed ΔXF plants with both construct. These plants are currently being propagated to bring them to homozygosity. It is hope in a future that they will be established as a new and valuable expression platform for better protein sialylation.

6 References

Aggarwal, S. (2011). What's fueling the biotech engine--2010 to 2011. Nature biotechnology **29,** 1083-1089.

Anthony, R.M., and Ravetch, J.V. (2010). A novel role for the IgG Fc glycan: the anti-inflammatory activity of sialylated IgG Fcs. Journal of clinical immunology **30 Suppl 1,** S9-14.

Anthony, R.M., Nimmerjahn, F., Ashline, D.J., Reinhold, V.N., Paulson, J.C., and Ravetch, J.V. (2008). Recapitulation of IVIG anti-inflammatory activity with a recombinant IgG Fc. Science **320,** 373-376.

Apweiler, R., Hermjakob, H., and Sharon, N. (1999). On the frequency of protein glycosylation, as deduced from analysis of the SWISS-PROT database. Biochimica et biophysica acta **1473,** 4-8.

Bakker, H., Rouwendal, G.J., Karnoup, A.S., Florack, D.E., Stoopen, G.M., Helsper, J.P., van Ree, R., van Die, I., and Bosch, D. (2006). An antibody produced in tobacco expressing a hybrid beta-1,4-galactosyltransferase is essentially devoid of plant carbohydrate epitopes. Proceedings of the National Academy of Sciences of the United States of America **103,** 7577-7582.

Bakker, H., Bardor, M., Molthoff, J.W., Gomord, V., Elbers, I., Stevens, L.H., Jordi, W., Lommen, A., Faye, L., Lerouge, P., and Bosch, D. (2001). Galactose-extended glycans of antibodies produced by transgenic plants. Proceedings of the National Academy of Sciences of the United States of America **98,** 2899-2904.

Bardor, M., Faveeuw, C., Fitchette, A.C., Gilbert, D., Galas, L., Trottein, F., Faye, L., and Lerouge, P. (2003). Immunoreactivity in mammals of two typical plant glyco-epitopes, core alpha(1,3)-fucose and core xylose. Glycobiology **13,** 427-434.

Boes, M., Prodeus, A.P., Schmidt, T., Carroll, M.C., and Chen, J. (1998). A critical role of natural immunoglobulin M in immediate defense against systemic bacterial infection. The Journal of experimental medicine **188,** 2381-2386.

Bosch, D., Castilho, A., Loos, A., Schots, A., and Steinkellner, H. (2013). N-glycosylation of plant-produced recombinant proteins. Current pharmaceutical design **19,** 5503-5512.

Burton, D.R., and Dwek, R.A. (2006). Immunology. Sugar determines antibody activity. Science **313,** 627-628.

Carrasco-Moro, R., Garcia-Navarrete, E., Navas-Garcia, M., Llano, M.A., and Sola, R.G. (2009). [Cavernous haemangioma of the skull]. Neurocirugia **20,** 559-562.

Castilho, A., and Steinkellner, H. (2012). Glyco-engineering in plants to produce human-like N-glycan structures. Biotechnology journal **7,** 1088-1098.

Castilho, A., Neumann, L., Daskalova, S., Mason, H.S., Steinkellner, H., Altmann, F., and Strasser, R. (2012). Engineering of sialylated mucin-type O-glycosylation in plants. The Journal of biological chemistry **287,** 36518-36526.

Castilho, A., Windwarder, M., Gattinger, P., Mach, L., Strasser, R., Altmann, F., and Steinkellner, H. (2014). Proteolytic and N-glycan processing of human alpha1-antitrypsin expressed in Nicotiana benthamiana. Plant physiology **166,** 1839-1851.

Castilho, A., Gruber, C., Thader, A., Oostenbrink, C., Pechlaner, M., Steinkellner, H., and Altmann, F. (2015). Processing of complex N-glycans in IgG Fc-region is affected by core fucosylation. mAbs**,** 0.

Castilho, A., Bohorova, N., Grass, J., Bohorov, O., Zeitlin, L., Whaley, K., Altmann, F., and Steinkellner, H. (2011a). Rapid high yield production of different glycoforms of Ebola virus monoclonal antibody. PloS one **6,** e26040.

Castilho, A., Neumann, L., Gattinger, P., Strasser, R., Vorauer-Uhl, K., Sterovsky, T., Altmann, F., and Steinkellner, H. (2013). Generation of biologically active multi-sialylated recombinant human EPOFc in plants. PloS one **8,** e54836.

Castilho, A., Gattinger, P., Grass, J., Jez, J., Pabst, M., Altmann, F., Gorfer, M., Strasser, R., and Steinkellner, H. (2011b). N-glycosylation engineering of plants for the biosynthesis of glycoproteins with bisected and branched complex N-glycans. Glycobiology **21,** 813-823.

Castilho, A., Strasser, R., Stadlmann, J., Grass, J., Jez, J., Gattinger, P., Kunert, R., Quendler, H., Pabst, M., Leonard, R., Altmann, F., and Steinkellner, H. (2010). In planta protein sialylation through overexpression of the respective mammalian pathway. The Journal of biological chemistry **285,** 15923-15930.

Chung, S.M., Frankman, E.L., and Tzfira, T. (2005). A versatile vector system for multiple gene expression in plants. Trends in plant science **10,** 357-361.

Dimitrov, J.D., Bayry, J., Siberil, S., and Kaveri, S.V. (2007). Sialylated therapeutic IgG: a sweet remedy for inflammatory diseases? Nephrology, dialysis, transplantation : official publication of the European Dialysis and Transplant Association - European Renal Association **22,** 1301-1304.

Dirnberger, D., Steinkellner, H., Abdennebi, L., Remy, J.J., and van de Wiel, D. (2001). Secretion of biologically active glycoforms of bovine follicle stimulating hormone in plants. European journal of biochemistry / FEBS **268,** 4570-4579.

Forsgren, A., and Sjoquist, J. (1966). "Protein A" from S. aureus. I. Pseudo-immune reaction with human gamma-globulin. Journal of immunology **97,** 822-827.

Forthal, D.N., Gach, J.S., Landucci, G., Jez, J., Strasser, R., Kunert, R., and Steinkellner, H. (2010). Fc-glycosylation influences Fcgamma receptor binding and cell-mediated anti-HIV activity of monoclonal antibody 2G12. Journal of immunology **185,** 6876-6882.

Gagnon, P. (2009). Monoclonal antibody purification with hydroxyapatite. New biotechnology **25,** 287-293.

Garcia-Gonzalez, M., Bettinger, S., Ott, S., Olivier, P., Kadouche, J., and Pouletty, P. (1988). Purification of murine IgG3 and IgM monoclonal antibodies by euglobulin precipitation. Journal of immunological methods **111,** 17-23.

Giritch, A., Marillonnet, S., Engler, C., van Eldik, G., Botterman, J., Klimyuk, V., and Gleba, Y. (2006). Rapid high-yield expression of full-size IgG antibodies in plants coinfected with noncompeting viral vectors. Proceedings of the National Academy of Sciences of the United States of America **103,** 14701-14706.

Gleba, Y., Klimyuk, V., and Marillonnet, S. (2007). Viral vectors for the expression of proteins in plants. Current opinion in biotechnology **18,** 134-141.

Gleba, Y.Y., Tuse, D., and Giritch, A. (2014). Plant Viral Vectors for Delivery by Agrobacterium. Curr Top Microbiol **375,** 155-192.

Gomord, V., Fitchette, A.C., Menu-Bouaouiche, L., Saint-Jore-Dupas, C., Plasson, C., Michaud, D., and Faye, L. (2010). Plant-specific glycosylation patterns in the context of therapeutic protein production. Plant biotechnology journal **8,** 564-587.

Hasnat, A., Bichenkova, E., Yu, X., Arnold, J.R., Fisher, J., Fedorova, O., and Andrews, J. (2007). Fluorescence spectroscopic and (19)f NMR studies of human thymidylate synthase with its cognate RNA. Journal of biomolecular structure & dynamics **25,** 253-270.

Jefferis, R. (2006). A sugar switch for anti-inflammatory antibodies. Nature biotechnology **24,** 1230-1231.

Jefferis, R. (2012). Isotype and glycoform selection for antibody therapeutics. Archives of biochemistry and biophysics **526,** 159-166.

Jez, J., Castilho, A., Grass, J., Vorauer-Uhl, K., Sterovsky, T., Altmann, F., and Steinkellner, H. (2013). Expression of functionally active sialylated human erythropoietin in plants. Biotechnology journal **8,** 371-382.

Kanda, Y., Yamada, T., Mori, K., Okazaki, A., Inoue, M., Kitajima-Miyama, K., Kuni-Kamochi, R., Nakano, R., Yano, K., Kakita, S., Shitara, K., and Satoh, M. (2007). Comparison of biological activity among nonfucosylated therapeutic IgG1 antibodies with three different N-linked Fc oligosaccharides: the high-mannose, hybrid, and complex types. Glycobiology **17,** 104-118.

Kaneko, Y., Nimmerjahn, F., and Ravetch, J.V. (2006). Anti-inflammatory activity of immunoglobulin G resulting from Fc sialylation. Science **313,** 670-673.

Klimyuk, V., Pogue, G., Herz, S., Butler, J., and Haydon, H. (2014). Production of recombinant antigens and antibodies in Nicotiana benthamiana using 'magnifection'

technology: GMP-compliant facilities for small- and large-scale manufacturing. Current topics in microbiology and immunology **375,** 127-154.

Kobata, A. (2008). The N-linked sugar chains of human immunoglobulin G: their unique pattern, and their functional roles. Biochimica et biophysica acta **1780,** 472-478.

Liebminger, E., Veit, C., Pabst, M., Batoux, M., Zipfel, C., Altmann, F., Mach, L., and Strasser, R. (2011). Beta-N-acetylhexosaminidases HEXO1 and HEXO3 are responsible for the formation of paucimannosidic N-glycans in Arabidopsis thaliana. The Journal of biological chemistry **286,** 10793-10802.

Lin, C.W., Tsai, M.H., Li, S.T., Tsai, T.I., Chu, K.C., Liu, Y.C., Lai, M.Y., Wu, C.Y., Tseng, Y.C., Shivatare, S.S., Wang, C.H., Chao, P., Wang, S.Y., Shih, H.W., Zeng, Y.F., You, T.H., Liao, J.Y., Tu, Y.C., Lin, Y.S., Chuang, H.Y., Chen, C.L., Tsai, C.S., Huang, C.C., Lin, N.H., Ma, C., Wu, C.Y., and Wong, C.H. (2015). A common glycan structure on immunoglobulin G for enhancement of effector functions. Proceedings of the National Academy of Sciences of the United States of America **112,** 10611-10616.

Loos, A., and Steinkellner, H. (2012). IgG-Fc glycoengineering in non-mammalian expression hosts. Archives of biochemistry and biophysics **526,** 167-173.

Loos, A., and Steinkellner, H. (2014). Plant glyco-biotechnology on the way to synthetic biology. Frontiers in plant science **5,** 523.

Loos, A., and Castilho, A. (2015). Transient Glyco-Engineering of N. benthamiana Aiming at the Synthesis of Multi-antennary Sialylated Proteins. Methods in molecular biology **1321,** 233-248.

Loos, A., Gruber, C., Altmann, F., Mehofer, U., Hensel, F., Grandits, M., Oostenbrink, C., Stadlmayr, G., Furtmuller, P.G., and Steinkellner, H. (2014). Expression and glycoengineering of functionally active heteromultimeric IgM in plants. Proceedings of the National Academy of Sciences of the United States of America **111,** 6263-6268.

Mohorko, E., Glockshuber, R., and Aebi, M. (2011). Oligosaccharyltransferase: the central enzyme of N-linked protein glycosylation. Journal of inherited metabolic disease **34,** 869-878.

Musiychuk, K., Sivalenka, R., Jaje, J., Bi, H., Flores, R., Shaw, B., Jones, R.M., Golovina, T., Schnipper, J., Khandker, L., Sun, R., Li, C., Kang, L., Voskinarian-Berse, V., Zhang, X., Streatfield, S., Hambor, J., Abbot, S., and Yusibov, V. (2013). Plant-produced human recombinant erythropoietic growth factors support erythroid differentiation in vitro. Stem cells and development **22,** 2326-2340.

Nagels, B., Weterings, K., Callewaert, N., and Van Damme, E.J.M. (2012). Production of Plant Made Pharmaceuticals: From Plant Host to Functional Protein. Crit Rev Plant Sci **31,** 148-180.

Okazaki, A., Shoji-Hosaka, E., Nakamura, K., Wakitani, M., Uchida, K., Kakita, S., Tsumoto, K., Kumagai, I., and Shitara, K. (2004). Fucose depletion from human IgG1 oligosaccharide enhances binding enthalpy and association rate between IgG1 and FcgammaRIIIa. Journal of molecular biology **336,** 1239-1249.

Pabst, M., Kuster, S.K., Wahl, F., Krismer, J., Dittrich, P.S., and Zenobi, R. (2015). A Microarray-Matrix-assisted Laser Desorption/Ionization-Mass Spectrometry Approach for Site-specific Protein N-glycosylation Analysis, as Demonstrated for Human Serum Immunoglobulin M (IgM). Molecular & cellular proteomics : MCP **14,** 1645-1656.

Palacpac, N.Q., Yoshida, S., Sakai, H., Kimura, Y., Fujiyama, K., Yoshida, T., and Seki, T. (1999). Stable expression of human beta1,4-galactosyltransferase in plant cells modifies N-linked glycosylation patterns. Proceedings of the National Academy of Sciences of the United States of America **96,** 4692-4697.

Prados, M.B., La Blunda, J., Szekeres-Bartho, J., Caramelo, J., and Miranda, S. (2011). Progesterone induces a switch in oligosaccharyltransferase isoform expression: consequences on IgG N-glycosylation. Immunology letters **137,** 28-37.

Roth, J., Zuber, C., Park, S., Jang, I., Lee, Y., Kysela, K.G., Le Fourn, V., Santimaria, R., Guhl, B., and Cho, J.W. (2010). Protein N-glycosylation, protein folding, and protein quality control. Molecules and cells **30,** 497-506.

Rudnicka, D., Oszmiana, A., Finch, D.K., Strickland, I., Schofield, D.J., Lowe, D.C., Sleeman, M.A., and Davis, D.M. (2013). Rituximab causes a polarization of B cells that augments its therapeutic function in NK-cell-mediated antibody-dependent cellular cytotoxicity. Blood **121,** 4694-4702.

Rybicki, E.P. (2010). Plant-made vaccines for humans and animals. Plant biotechnology journal **8,** 620-637.

Samyn-Petit, B., Wajda Dubos, J.P., Chirat, F., Coddeville, B., Demaizieres, G., Farrer, S., Slomianny, M.C., Theisen, M., and Delannoy, P. (2003). Comparative analysis of the site-specific N-glycosylation of human lactoferrin produced in maize and tobacco plants. European journal of biochemistry / FEBS **270,** 3235-3242.

Scallon, B.J., Tam, S.H., McCarthy, S.G., Cai, A.N., and Raju, T.S. (2007). Higher levels of sialylated Fc glycans in immunoglobulin G molecules can adversely impact functionality. Molecular immunology **44,** 1524-1534.

Schahs, M., Strasser, R., Stadlmann, J., Kunert, R., Rademacher, T., and Steinkellner, H. (2007). Production of a monoclonal antibody in plants with a humanized N-glycosylation pattern. Plant biotechnology journal **5,** 657-663.

Schiestl, M., Stangler, T., Torella, C., Cepeljnik, T., Toll, H., and Grau, R. (2011). Acceptable changes in quality attributes of glycosylated biopharmaceuticals. Nature biotechnology **29,** 310-312.

Schneider, J.D., Castilho, A., Neumann, L., Altmann, F., Loos, A., Kannan, L., Mor, T.S., and Steinkellner, H. (2014a). Expression of human butyrylcholinesterase with an engineered glycosylation profile resembling the plasma-derived orthologue. Biotechnology journal **9,** 501-510.

Schneider, J.D., Marillonnet, S., Castilho, A., Gruber, C., Werner, S., Mach, L., Klimyuk, V., Mor, T.S., and Steinkellner, H. (2014b). Oligomerization status influences subcellular deposition and glycosylation of recombinant butyrylcholinesterase in Nicotiana benthamiana. Plant Biotechnol J **12,** 832-839.

Schoberer, J., Liebminger, E., Vavra, U., Veit, C., Castilho, A., Dicker, M., Maresch, D., Altmann, F., Hawes, C., Botchway, S.W., and Strasser, R. (2014). The transmembrane domain of N -acetylglucosaminyltransferase I is the key determinant for its Golgi subcompartmentation. The Plant journal : for cell and molecular biology **80,** 809-822.

Schwarz, F., and Aebi, M. (2011). Mechanisms and principles of N-linked protein glycosylation. Current opinion in structural biology **21,** 576-582.

Shaaltiel, Y., Bartfeld, D., Hashmueli, S., Baum, G., Brill-Almon, E., Galili, G., Dym, O., Boldin-Adamsky, S.A., Silman, I., Sussman, J.L., Futerman, A.H., and Aviezer, D. (2007). Production of glucocerebrosidase with terminal mannose glycans for enzyme replacement therapy of Gaucher's disease using a plant cell system. Plant biotechnology journal **5,** 579-590.

Shi, X., and Jarvis, D.L. (2007). Protein N-glycosylation in the baculovirus-insect cell system. Current drug targets **8,** 1116-1125.

Shields, R.L., Lai, J., Keck, R., O'Connell, L.Y., Hong, K., Meng, Y.G., Weikert, S.H., and Presta, L.G. (2002). Lack of fucose on human IgG1 N-linked oligosaccharide improves binding to human Fcgamma RIII and antibody-dependent cellular toxicity. The Journal of biological chemistry **277,** 26733-26740.

Shinkawa, T., Nakamura, K., Yamane, N., Shoji-Hosaka, E., Kanda, Y., Sakurada, M., Uchida, K., Anazawa, H., Satoh, M., Yamasaki, M., Hanai, N., and Shitara, K. (2003). The absence of fucose but not the presence of galactose or bisecting N-acetylglucosamine of human IgG1 complex-type oligosaccharides shows the critical role of enhancing antibody-dependent cellular cytotoxicity. The Journal of biological chemistry **278,** 3466-3473.

Sola, R.J., and Griebenow, K. (2010). Glycosylation of therapeutic proteins: an effective strategy to optimize efficacy. BioDrugs : clinical immunotherapeutics, biopharmaceuticals and gene therapy **24,** 9-21.
Spiegelberg, H.L. (1989). Biological role of different antibody classes. International archives of allergy and applied immunology **90 Suppl 1,** 22-27.
Stadlmann, J., Pabst, M., Kolarich, D., Kunert, R., and Altmann, F. (2008). Analysis of immunoglobulin glycosylation by LC-ESI-MS of glycopeptides and oligosaccharides. Proteomics **8,** 2858-2871.
Steinkellner, H., and Castilho, A. (2015). N-Glyco-Engineering in Plants: Update on Strategies and Major Achievements. Methods in molecular biology **1321,** 195-212.
Stoger, E., Fischer, R., Moloney, M., and Ma, J.K. (2014). Plant molecular pharming for the treatment of chronic and infectious diseases. Annual review of plant biology **65,** 743-768.
Strasser, R., Altmann, F., and Steinkellner, H. (2014). Controlled glycosylation of plant-produced recombinant proteins. Current opinion in biotechnology **30,** 95-100.
Strasser, R., Altmann, F., Mach, L., Glossl, J., and Steinkellner, H. (2004). Generation of Arabidopsis thaliana plants with complex N-glycans lacking beta1,2-linked xylose and core alpha1,3-linked fucose. FEBS letters **561,** 132-136.
Strasser, R., Bondili, J.S., Schoberer, J., Svoboda, B., Liebminger, E., Glossl, J., Altmann, F., Steinkellner, H., and Mach, L. (2007). Enzymatic properties and subcellular localization of Arabidopsis beta-N-acetylhexosaminidases. Plant physiology **145,** 5-16.
Strasser, R., Stadlmann, J., Schahs, M., Stiegler, G., Quendler, H., Mach, L., Glossl, J., Weterings, K., Pabst, M., and Steinkellner, H. (2008). Generation of glyco-engineered Nicotiana benthamiana for the production of monoclonal antibodies with a homogeneous human-like N-glycan structure. Plant biotechnology journal **6,** 392-402.
Strasser, R., Castilho, A., Stadlmann, J., Kunert, R., Quendler, H., Gattinger, P., Jez, J., Rademacher, T., Altmann, F., Mach, L., and Steinkellner, H. (2009). Improved virus neutralization by plant-produced anti-HIV antibodies with a homogeneous beta1,4-galactosylated N-glycan profile. The Journal of biological chemistry **284,** 20479-20485.
Varki, A. (1993). Biological roles of oligosaccharides: all of the theories are correct. Glycobiology **3,** 97-130.
Vezina, L.P., Faye, L., Lerouge, P., D'Aoust, M.A., Marquet-Blouin, E., Burel, C., Lavoie, P.O., Bardor, M., and Gomord, V. (2009). Transient co-expression for fast and high-yield production of antibodies with human-like N-glycans in plants. Plant biotechnology journal **7,** 442-455.
Wang, P., Dong, S., Brailsford, J.A., Iyer, K., Townsend, S.D., Zhang, Q., Hendrickson, R.C., Shieh, J., Moore, M.A., and Danishefsky, S.J. (2012). At last: erythropoietin as a single glycoform. Angewandte Chemie **51,** 11576-11584.
Werner, S., Breus, O., Symonenko, Y., Marillonnet, S., and Gleba, Y. (2011). High-level recombinant protein expression in transgenic plants by using a double-inducible viral vector. Proceedings of the National Academy of Sciences of the United States of America **108,** 14061-14066.
Whaley, K.J., Hiatt, A., and Zeitlin, L. (2011). Emerging antibody products and Nicotiana manufacturing. Human vaccines **7,** 349-356.
Wilken, L.R., and Nikolov, Z.L. (2012). Recovery and purification of plant-made recombinant proteins. Biotechnology advances **30,** 419-433.
Winkler, S., Wilson, D., and Kaplan, D.L. (2000). Controlling beta-sheet assembly in genetically engineered silk by enzymatic phosphorylation/dephosphorylation. Biochemistry **39,** 12739-12746.
Zauner, G., Selman, M.H., Bondt, A., Rombouts, Y., Blank, D., Deelder, A.M., and Wuhrer, M. (2013). Glycoproteomic analysis of antibodies. Molecular & cellular proteomics : MCP **12,** 856-865.

Zeitlin, L., Pettitt, J., Scully, C., Bohorova, N., Kim, D., Pauly, M., Hiatt, A., Ngo, L., Steinkellner, H., Whaley, K.J., and Olinger, G.G. (2011). Enhanced potency of a fucose-free monoclonal antibody being developed as an Ebola virus immunoprotectant. Proceedings of the National Academy of Sciences of the United States of America **108,** 20690-20694.